Analyzing the Noise Behaviour of a Model Reference Adaptive Controller which uses Simultaneous Probing, Estimation, and Control

by

Chuan Yu

A thesis
presented to the University of Waterloo
in fulfillment of the
thesis requirement for the degree of
Master of Applied Science
in
Electrical and Computer Engineering

Waterloo, Ontario, Canada, 2012

I hereby declare that I am the sole author of this thesis. This is a true copy of the thesis, including any required final revisions, as accepted by my examiners.

I understand that my thesis may be made electronically available to the public.

Abstract

In classical model reference adaptive control, the goal is to design a controller to make the closed-loop system act like a prespecified stable reference model. A recent approach yields a linear periodic controller which simultaneously performs probing, estimation, and control. This linear controller is not only able to handle time-varying systems, but also provides exponential stability. In addition, from simulations, it is found that the controller has excellent noise rejection in certain cases.

In this thesis, we used the induced noise gain as the measurement of noise rejection. For plants that are minimum phase with relative degree one, we started with the case where the plant is first order and linear time-invariant. Then we moved to the case where the plant is first order and linear time-varying. Finally, we extended to the general case where the plant is linear time-varying with relative degree one. For the above cases, we quantitatively investigated how certain control parameters affect the induced noise gain.

Acknowledgements

I would like to thank my supervisor, Professor Daniel Miller, who was abundantly helpful and offered invaluable guidance and instructions. Without his outstanding method to approach and analyze problems, this research would not have been possible. I would also like to thank Darrell Gaudette and Hunter Song for having technical discussions with me and giving advice to me. In addition, I would also want to thank my dearly-loved family for their unwavering support throughout my student life.

Dedication

This is dedicated to my wonderful family
and
my beloved girlfriend, Pei Huang.

Table of Contents

List of Tables

List of Figures

Chapter 1

Introduction

1.1 Background

The objective of adaptive control is to deal with plants with unknown or time-varying parameters. The basic idea is to have a controller which tunes itself to the plant being controlled. An adaptive controller typically consists of a LTI compensator and a turning mechanism, which adjusts the compensator gains to match the plant [3]. Because of the modification law, a typical adaptive controller is nonlinear. One of the fundamental concepts of classical adaptive control is based on the use of parameter estimations. Common methods of estimation include Least Squares Algorithm and Gradient Algorithm from Goodwin and Sin [5]. Both of these methods provide update laws which estimate the plant parameters in real time. From the estimated plant parameters, the controller then generates the control signal to the use of the plant.

One of the most important problems of adaptive control is the Model Reference Adaptive Control Problem (MRACP). This was first suggested by Whitaker [6] to solve the autopilot control problem in the early 1950's. However, the proof of global stability was not completed until 1978-1980 [7,8,9,10]. In MRACP, the goal is to have the output of the plant asymptotically track the output of a stable reference model in response to a piecewise continuous bounded input. To solve the MRACP, classical assumptions on the plant model are:

i) the plant is minimum phase;

ii) an upper bound on the plant order is known;

iii) the plant relative degree is known;

iv) the sign of the high-frequency gain is known.

Later work has shown that iii) can be leveraged to require only the upper bound of the relative degree of the plant [11] and iv) can be removed [12]. Based on these results, many adaptive controllers were build during the period of 1980 to 2000 [13][14][15][16][17]. However, most controllers suffer from some of the following problems:

i) the controller cannot track time-varying system well;

ii) poor transient behavior - only asymptotic results are proved;

iii) the controller is often highly nonlinear, so the effect of initial conditions and the input are coupled;

iv) system typically requires large control signal.

To solve the above problems, a new approach to MRACP was presented in [3]. This approach is based on a linear sampled-data periodic control. Different from other adaptive controllers, this controller directly estimates the control signal rather than estimating the plant parameters. The intuition is from the fact that generating the desired control signal is the ultimate goal. This controller is periodic; it divides each control period into estimation phase and control phase, and performs estimation and control sequentially. This linear adaptive controller has greatly improved all the aforementioned undesirable properties. In addition, due to the fact that this controller is linear, the closed-loop system has tolerance to unmodelled dynamics. Of course, there is no free lunch. This controller also has the following weaknesses:

i) control signals are rapidly varying in each control period, which may require fast actuators for real implementation;

ii) to achieve optimal tracking, a small sampling period is used, which leads to large controller gains and poor noise tolerance.

Using the same type of idea, [1] cleverly redesigned the controller of [3][1]. Rather than sequentially doing estimation and control in each control period, the modified controller

[1]In this thesis, we will refer the original LPC (linear periodic controller) to the controller designed in [3] and the redesigned LPC as the one purposed in [1].

simultaneously performs estimation and control [2]. With the modification, the control signal is much less erratic. Similar to the controller presented in [3], exponential convergence results are proven for the redesigned controller. This ensures immediate tracking as opposed to asymptotic convergence. In addition, compared to the original controller, the redesigned controller allows the use of a much larger sampling period for the same level of performance.

Another nice side-effect is that the redesigned controller improves the noise tolerance. If the high frequency gain is assumed to be known, simulations show that noise has only a minor effect for a first order time-varying system. Furthermore, for a first order LTI plant, simulations indicate that the induced noise gain converges to a modest value as the sampling period goes to zero. On the other hand, simulation from [18] shows that the noise gain is large for a relative degree two system.

1.2 Objectives

The objective of this thesis is to investigate the noise behavior of the controller proposed in [1]. From the simulations, nice noise behavior has been observed for some particular plants. Of course, this is not enough to say that the noise is well behaved; we are not sure under which conditions noise is going to behave well. Hence, our first objective is to investigate the noise gain for different types of plants. This includes first order LTI plants, first order time-varying plants, relative degree one time-varying plants, and relative degree n time-varying plants[3]. For each type of plants, we would like to find an expression for the induced noise gain as a function of the sampling period.

Next, we should focus on how to improve the noise behavior. In other words, we would seek a way to reduce the induced noise gain. If we have an expression of the induced noise gain, we should be able to see which parameters affect the induced noise gain, and hence find a way to reduce it.

1.3 Achievements

We started with the simplest plant, a first order LTI plant and derived expressions for the induced noise gain. It was found that the induced noise gain is small for any relative degree

[2]Most classical adaptive controllers performs estimation and control simultaneously.

[3]In this thesis, we did not show any result for the case where the plant is relative degree $n > 1$ and time-varying. This is because the noise gain appears to be large from simulation results and no constructive result was found to reduce the noise gain.

one plant. Moreover, we found that if the free controller parameters are chosen properly, the induced noise gain converges to one as the sampling period tends to zero. This result is consistent with the previous simulations, and is definitely a desirable feature.

1.4 Overview of Thesis

The outline of this thesis is as follows. The next chapter presented some preliminary mathematics. The problem setup was presented in Chapter 3. Starting from the simplest case, in Chapter 4, we found an upper bound of the induced noise gain for first order LTI plants. In Chapter 5, a similar result was derived for first order linear time-varying plants. Finally, in Chapter 6, we leveraged the previous results and found a bound of the induced noise gain for relative degree one plants. In Chapter 4, 5, and 6, we presented detailed proofs of the bound of the induced noise gain as well as simulations supporting the related results. Concluding remarks, the main result, and possible future work is provided in Chapter 7.

Chapter 2

Mathematical Preliminaries

Let $\mathbb{Z}$ denote the set of integers, $\mathbb{Z}^+$ denote the set of non-negative integers, $\mathbb{N}$ denote the set of positive integers, $\mathbb{R}$ denote the set of real numbers, $\mathbb{R}^+$ denote the set of non-negative real numbers, $\mathbb{C}$ denote the set of complex numbers, and $\mathbb{C}^-$ denote the set of complex numbers with a real part less than zero.

We use the Euclidean norm of vector $x \in \mathbb{R}^n$ to measure its size: $||x|| := (\sum_{i=1}^{n} x_i^2)^{\frac{1}{2}}$. For a real-valued matrix $A \in \mathbb{R}^{n\times m}$, we use the corresponding induced norm to measure its size:

$$||A|| = \sup_{||x||=1} \frac{||Ax||}{||x||}.$$

We let $PC(\mathbb{R}^{n\times m})$ denote the set of piecewise continuous functions from $\mathbb{R}^+$ to $\mathbb{R}^{n\times m}$. For function $f \in PC(\mathbb{R}^{n\times m})$, define

$$||f||_\infty := \sup_{t\in\mathbb{R}^+} ||f(t)||.$$

Let $PC_\infty(\mathbb{R}^{n\times m})$ denote the set of $f \in PC(\mathbb{R}^{n\times m})$ for which $\|f\|_\infty < \infty$. To reduce clutter, we drop the $\mathbb{R}^{n\times m}$ and simply write PC and PC_∞. We let $PS(\mathbb{R}^{n\times m})$ denote the set of *piecewise smooth* elements of $PC(\mathbb{R}^{n\times m})$. We let $PS_\infty(\mathbb{R}^{n\times m})$ denote the set of $f \in PS(\mathbb{R}^{n\times m})$ for which $\|f\|_\infty < \infty$ and $\|\dot{f}\|_\infty < \infty$. With $T > 0$, we let $PS(\mathbb{R}^{n\times m}, T)$ denote the set of $f \in PS(R^{n\times m})$ for which every discontinuity of $\begin{bmatrix} f \\ \dot{f} \end{bmatrix}$ are at least T time units apart, and we define $PS_\infty(\mathbb{R}^{n\times m}, T)$ in an analogous way. Henceforth, when the dimension is clear from the context, we drop the $\mathbb{R}^{n\times m}$ and simply write PS, PS_∞, $PS(T)$, and $PS_\infty(T)$.

In this paper, we will deal with time-varying systems, and it will be convenient to discuss the gain of such a system when the initial condition at time zero is zero. To this end, the gain of G: $PC_\infty \to PC$ is defined by

$$\|G\| := \sup\left\{ \frac{\|Gu_m\|_\infty}{\|u_m\|_\infty} : u_m \in PC_\infty, \|u_m\|_\infty \neq 0 \right\}.$$

We say that $f : \mathbb{R}^+ \to \mathbb{R}^{n\times m}$ is of order T^j, and write $f = \mathcal{O}(T^j)$, if there exist constants $c_1 > 0$ and $T_1 > 0$ so that

$$\|f(T)\| \leq c_1 T^j, \;\; T \in (0, T_1).$$

If the function f does not only depend on $T > 0$ but also depends implicitly on a variable $\bar{\theta}$ restricted to a set $\bar{\mathcal{P}} \subset PS$, we say that $f = \mathcal{O}(T^j)$ if there exist constants $c_1 > 0$ and $T_1 > 0$ so that

$$\|f(T)\| \leq c_1 T^j, \;\; T \in (0, T_1), \quad \bar{\theta} \in \bar{\mathcal{P}}.$$

There are many places in this thesis where we use the Taylor Series with order notation. We say that for $T > 0$ and $a \in \mathbb{R}$,

$$e^{aT} = \; 1 + aT + \mathcal{O}(T^2).$$

Chapter 3

Problem Formulation

3.1 Generalized Plant

In both [1] and [3], the controller design process starts with a classical input-output model which is in terms of an auxiliary variable η. With $(D^i f)(t) := \frac{d^i f}{dt^i}(t)$, consider

$$\begin{array}{rcl} \sum_{i=0}^{n} a_i(t) D^i \eta & = & g(t)u, \\ y & = & \sum_{i=0}^{n-m} b_i(t) D^i \eta, \end{array} \tag{3.1}$$

where the variables are normalized so that $a_n = b_{n-m} = 1$. If the parameters are constant, then the transfer function is given by $g\frac{\sum_{i=0}^{n-m} b_i s^i}{\sum_{i=0}^{n} a_i s^i}$, where g represents the high frequency gain and m represents the relative degree. Under some reasonable assumptions, the above can be modelled using the single-input single-output (SISO) linear time-varying plant P, which is described by:

$$\begin{array}{rcl} \dot{x}(t) & = & A(t)x(t) + B(t)u(t), \quad x(t_0) = x_0, \\ y(t) & = & C(t)x(t), \end{array} \tag{3.2}$$

with $x(t) \in \mathbb{R}^n$ being the plant state, $u(t) \in \mathbb{R}$ being the plant input, and $y(t) \in \mathbb{R}$ being the plant output. Since we allow a good deal of model uncertainties, we let $\mathcal{P}$ denote the set of admissible models[1].

The stable SISO reference model P_m is described by:

$$\begin{array}{rcl} \dot{x}_m & = & A_m x_m + B_m u_m, \; x_m(t_0) = x_{m_0}, \\ y_m & = & C_m x_m, \end{array} \tag{3.3}$$

[1]The list of assumptions and the definition of $\mathcal{P}$ are described more precisely in the later sections.

with $x_m(t) \in \mathbb{R}^{n_m}$ being the state, $u_m(t) \in \mathbb{R}$ being the reference model input, and $y_m(t) \in \mathbb{R}$ being the reference model output. The reference model is chosen to have desired behavior of the close loop system. Hence, the control objective is to let the plant output track the reference output. So, we define the tracking error by

$$e(t) := y_m(t) - y(t).$$

Since the designed controller is a sampled data controller, which periodically samples an external modeled input u_m, an anti-aliasing filter is applied before sampling u_m. The anti-aliasing filter is

$$\dot{\bar{u}}_m = -\sigma \bar{u}_m + \sigma u_m,\ \bar{u}_m(t_0) = \bar{u}_{m_0}, \tag{3.4}$$

and $\sigma > 0$. In the following sections, we denote the anti-aliasing map as F_α. With the use of the anti-aliasing filter, the reference model is updated to:

$$\begin{array}{rcl} \dot{\bar{x}}_m & = & A_m \bar{x}_m + B_m \bar{u}_m,\ \bar{x}_m(t_0) = x_{m_0}, \\ \bar{y}_m & = & C_m \bar{x}_m, \end{array} \tag{3.5}$$

which the input-output map of the updated reference model is labeled $\bar{P}_m$. We also define the associated tracking error by

$$\bar{e}(t) := \bar{y}_m(t) - y(t). \tag{3.6}$$

We consider the following class of sampled-data compensators:

$$\begin{array}{rcl} z[k+1] & = & F(k)z[k] + G(k)y(kh) + H(k)\bar{x}_m(kh) + J(k)\bar{u}_m(kh), z[k_0] = z_0 \in \mathbb{R}^l, \\ u(kh+\tau) & = & L(k)z[k] + M(k)y(kh), \tau \in [0, h), \end{array} \tag{3.7}$$

whose input-output map is labeled K (with $z_0 = 0$) and whose gains F, G, H, J, L and M are periodic of period $p \in \mathbb{N}$. The period of the controller is $T := ph$, and we represent this controller by (F, G, H, J, L, M, h, p). Observe that (3.7) can be implemented with a sampler, a zero-order-hold, and an l^{th} order periodically time-varying discrete-time system of period p. The control schematic is shown in Figure 3.1.

Note that the controller is a combination of discrete and continuous subsystems. Hence, the closed-loop states are a mixture of discrete and continuous states. This is defined by

$$x_{sd}(t) := \begin{bmatrix} x(t) \\ \bar{x}_m(t) \\ \bar{u}_m(t) \\ z[k] \end{bmatrix}, \quad t \in [kh, (k+1)h).$$

Now, we borrow the notion of stability from [3].

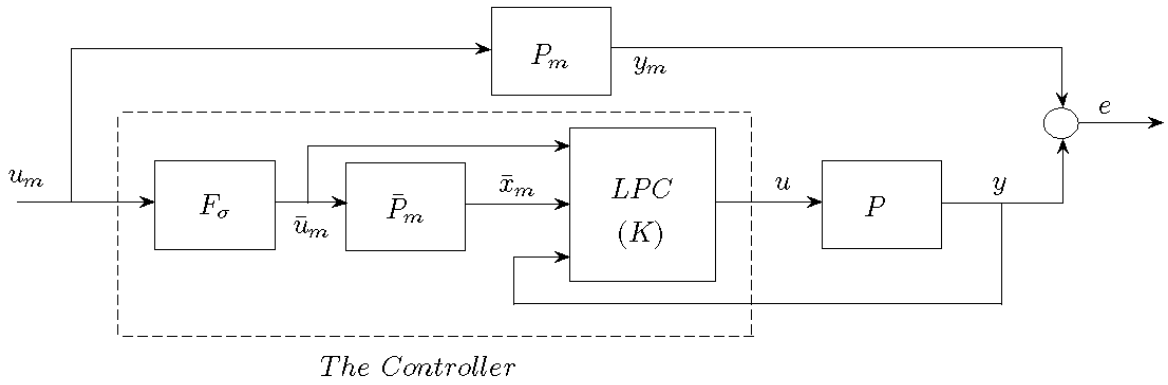

Figure 3.1: The Feedback Diagram

Definition 1. *The controller (3.4), (3.5), and (3.6) exponentially stabilizes $\mathcal{P}$ if there exist constants $\gamma > 0$ and $\lambda < 0$ so that, for every $P \in \mathcal{P}$, set of initial conditions x_0, $\bar{x}_{m_0}$, $\bar{u}_{m_0}$, and z_0, set of initial times $k_0 \in \mathbb{Z}^+$ and $t_0 = k_0 h$, with $u_m(t) = 0$ for $t \geq t_0$ we have*

$$\|x_{sd}(t)\| \leq \gamma e^{\lambda(t-t_0)}(\|x_0\| + \|\bar{x}_{m_0}\| + \|\bar{u}_{m_0}\| + \|z_0\|), \quad t \geq t_0.$$

Hence, for the reference plant, we can choose $\gamma_m > 0$ and $\lambda_m < 0$ such that $\|e^{A_m t}\| \leq \gamma_m e^{\lambda_m t}$. Since the stability is defined using the filtered input $\bar{u}_m$ rather than u_m (we are looking at the associated tracking error $\bar{e}$ instead of e), one might wonder how the anti-aliasing filter will affect the result. However, a result from [1] illustrated the transient behaviour of $|\bar{e}(t) - e(t)|$ - for $\sigma > \|A_m\|$ we have

$$|\bar{e}(t) - e(t)| = |\bar{y}_m(t) - y_m(t)| \leq \frac{\|B_m\| \cdot \|C_m\|}{\sigma - \|A_m\|}[(\gamma_m + 1)e^{\lambda_m t}|\bar{u}_{m_0}| +$$

$$(\gamma_m \frac{\|A_m\|}{|\lambda_m|} + 1)\|u_m\|_\infty], \quad t \geq 0. \tag{3.8}$$

Hence, by choosing a sufficiently large filter gain $\sigma > 0$, the difference between $\bar{e}$ and e can be made as small as desired.

Under some reasonable assumptions, it is shown in [3] that how to convert (3.1) to a state-space model with specially chosen states that isolate the zero dynamics. The underlying goal is to isolate the zero dynamics and try to control what is left. Here, we will only present the state space model with a list of assumptions on its parameters. If we

associate state w with the zero dynamics and state v with output y and its derivatives, such that

$$w := \begin{bmatrix} \eta \\ D\eta \\ \vdots \\ D^{n-m-1}\eta \end{bmatrix} \quad \text{and} \quad v := \begin{bmatrix} y \\ Dy \\ \vdots \\ D^{m-1}y \end{bmatrix}, \tag{3.9}$$

the state space representation of (3.1) is:

$$\begin{array}{rcl} \begin{bmatrix} \dot{w} \\ \dot{v} \end{bmatrix} & = & \begin{bmatrix} A_1(t) & b_1c_2 \\ b_2c_1(t) & A_2(t) \end{bmatrix} \begin{bmatrix} w \\ v \end{bmatrix} + \begin{bmatrix} 0 \\ g(t)b_2 \end{bmatrix} u, \\ y & = & \begin{bmatrix} 0 & c_2 \end{bmatrix} \begin{bmatrix} w \\ v \end{bmatrix}, \end{array} \tag{3.10}$$

with

$$\begin{array}{rcl} A_1(t) & := & \begin{bmatrix} & 1 & & \\ & & \ddots & \\ & & & 1 \\ -b_0(t) & -b_1(t) & \cdots & -b_{n-m-1}(t) \end{bmatrix}, b_1 = \begin{bmatrix} 0 \\ \vdots \\ 0 \\ 1 \end{bmatrix} \in \mathbb{R}^{n-m}, \\ A_2(t) & := & \begin{bmatrix} & 1 & & \\ & & \cdots & \\ & & & 1 \\ -\beta_0(t) & -\beta_1(t) & \cdots & -\beta_{m-1}(t) \end{bmatrix}, b_2 = \begin{bmatrix} 0 \\ \vdots \\ 0 \\ 1 \end{bmatrix} \in \mathbb{R}^{m}, \\ c_1(t) & = & \begin{bmatrix} \alpha_0(t) & \cdots & \alpha_{n-m-1}(t) \end{bmatrix}, c_2 = \begin{bmatrix} 1 & 0 & \cdots & 0 \end{bmatrix}. \end{array} \tag{3.11}$$

The above state-space model is parameterized by

$$\bar{\theta}(t) := \begin{bmatrix} \alpha_0(t) & \cdots & \alpha_{n-m-1}(t) & \beta_0(t) & \cdots & \beta_{m-1}(t) & b_0(t) & \cdots & b_{n-m-1}(t) & g(t) \end{bmatrix}^T, \tag{3.12}$$

which takes value in $\mathbb{R}^{2n-m+1}$.

The set of assumptions made on $\bar{\theta}(t)$ and the reference model are:

Assumptions:

- *Assumption* 1: (Compact set) There exists a compact set $\bar{\Gamma}$ so that $\bar{\theta}(t) \in \bar{\Gamma}$ for all $t \geq 0$.
- *Assumption* 2: (Infrequent jumps) There exists a $\bar{T}_0 > 0$ so that $\bar{\theta} \in PS_\infty(\bar{T}_0)$.
- *Assumption* 3: (Bounded derivative) There exists a constant $\bar{\mu}_1$ so that $\text{esssup}_{t\geq 0} \|\dot{\bar{\theta}}(t)\| \leq \bar{\mu}_1$ for all $t \geq 0$.
- *Assumption* 4: (Regularity of g) There exists a positive constant $\underline{g}$ so that $|g(t)| \geq \underline{g}$.
- *Assumption* 5: (Uniformly exponential stable zero dynamics) There exists a positive constant $\gamma_0 > 0$ and $\lambda_0 < 0$ so that the transition matrix Φ_{A_1} corresponding to A_1 satisfies

$$||\Phi_{A_1}(t, t_0)|| \leq \gamma_0 e^{\lambda_0(t-t_0)}, t \geq t_0 \geq 0.$$

Remark 1. *Since $\bar{\Gamma}$ is a compact set, then the biggest admissible value of g is well defined*

$$\bar{g} := \sup\{\bar{\theta}_{2n-m+1} : \bar{\theta} \in \bar{\Gamma}\}.$$

With the above assumptions, in [1], the set of plant uncertainties is presented to be of the form

$$\bar{\mathcal{P}}(n, m, \bar{\Gamma}, \bar{\mu}_1, \bar{T}_0, \underline{g}, \gamma_0, \lambda_0). \tag{3.13}$$

For every $n \geq m \geq 1$, compact set $\bar{\Gamma} \subset \mathbb{R}^{2n-m+1}$, set of positive constants $\bar{\mu}_1$, $\bar{T}_0$, $\underline{g}$, and γ_0 and negative constant λ_0, there exists a natural class of models of the form (3.14)-(3.11) that satisfies the listed assumptions.

Combine the plant - (3.10), the reference model - (3.5), and the anti-aliasing filter - (3.4), and define $\bar{x} := \begin{bmatrix} w \\ v \\ \bar{x}_m \\ \bar{u}_m \end{bmatrix}$; then the generalized plant is:

$$\begin{aligned} \dot{\bar{x}} &= \begin{bmatrix} A_1(t) & b_2c_2 & 0 & 0 \\ b_2c_1(t) & A_2(t) & 0 & 0 \\ 0 & 0 & A_m & B_m \\ 0 & 0 & 0 & -\sigma \end{bmatrix} \bar{x} + g(t) \begin{bmatrix} 0 \\ b_2 \\ 0 \\ 0 \end{bmatrix} u + \begin{bmatrix} 0 \\ 0 \\ 0 \\ \sigma \end{bmatrix} u_m, \\ \begin{bmatrix} y \\ \bar{e} \end{bmatrix} &= \begin{bmatrix} 0 & c_2 & 0 & 0 \\ 0 & -c_2 & C_m & 0 \end{bmatrix} \bar{x}. \end{aligned} \tag{3.14}$$

In addition, a natural assumption is made on the reference model:

- *Assumption* 6: The relative degree of the reference model is at least m.

3.2 The Ideal Controller

As mentioned previously, rather than estimating the plant parameters, the control signal is directly estimated in both [1] and [3]. Hence, the so-called ideal control signal is required. Here, we summarize how the ideal control law is constructed. To illustrate the idea, consider the first order linear time invariant system

$$\dot{y} = ay + gu. \tag{3.15}$$

The differential equation which describes the error $\bar{e} = \bar{y}_m - y$ is

$$(\dot{\bar{y}}_m - \dot{y}) = a_m(\bar{y}_m - y) + (b_m\bar{u}_m - gu + (a_m - a)y). \tag{3.16}$$

In practice, initial mis-matches between the reference model and plant exist. Here, if we wish to have the difference $\bar{e}$ decay to zero like $e^{a_m t}$, we should set

$$b_m\bar{u}_m - gu + (a_m - a)y = 0, \tag{3.17}$$

so that (3.16) becomes

$$\dot{\bar{e}} = a_m\bar{e}.$$

Hence, (3.17) suggests the ideal control law to be[2]

$$u^o = \frac{1}{g}\begin{bmatrix} a_m - a & 0 & b_m \end{bmatrix}\begin{bmatrix} y \\ \bar{y}_m \\ \bar{u}_m \end{bmatrix}.$$

Of course, for the general case, the derivation of the ideal control law is much more involved. Here we only present the result. First define

$$\Lambda_2 := \begin{bmatrix} & 1 & & \\ & & \ddots & \\ & & & 1 \\ 0 & 0 & \cdots & 0 \end{bmatrix}, \quad f_2(t) := \begin{bmatrix} \beta_0(t) & \cdots & \beta_{n-m-1}(t) \end{bmatrix}.$$

[2]We denoted the ideal control signal by $u^o(t)$.

Choose $\bar{f}_2$ so that $\bar{A}_2 = \Lambda_2 + b_2\bar{f}_2$ is stable and has eigenvalues with real parts less than λ_m. Using Assumption 6, we can choose $k_1 \in \mathbb{R}^{1\times n_m}$ and $k_2 \in \mathbb{R}$ so that

$$\frac{P_m(s)}{c_2(sI-\bar{A}_2)^{-1}b_2} = k_2 + k_1(sI - A_m)^{-1}B_m,$$

and we end up with the **ideal control law**

$$u^o(t) = \frac{1}{g(t)}\left[\begin{array}{cccc} -c_1(t) & \bar{f}_2 - f_2(t) & k_1 & k_2 \end{array}\right]\bar{x}(t). \tag{3.18}$$

3.3 The Redesigned LPC

In [3], the original design, the idea is to use small test signals to probe the system to obtain parameter estimation, and then apply the control signal based on the estimation. As a modified design, in [1], probing, estimation, and control are carried out simultaneously. To avoid repetition, the design procedure is omitted here. From Assumption 1 and 4, it follows that

$$\mathcal{G} := \left\{|g| \geq \underline{g} : \text{there exists a } \psi \in \mathbb{R}^{2n-m} \text{ so that } \left[\begin{array}{c}\psi\\ g\end{array}\right] \in \bar{\Gamma}\right\}$$

is a compact set which does not include zero. By the Stone-Weierstrass Approximation Theorem, for every $\varepsilon > 0$ there exists a $q \in N$ such that the polynomial $\hat{f}_\varepsilon(g) = \sum_{i=0}^{q} c_i g^i$ satisfies

$$\left|1 - g\hat{f}_\varepsilon(g)\right| < \varepsilon, \quad g \in \mathcal{G}. \tag{3.19}$$

In [1], the above approximation method is used to estimate the ideal control law. This will be elaborated more in the later sections. Now, define two $(m+1)\times(m+1)$ matrices and a vector:

$$S_m = \left[\begin{array}{ccccc} 1 & 0 & 0 & \cdots & 0\\ 1 & 1 & 1 & \cdots & 1\\ 1 & 2 & 2^2 & \cdots & 2^m\\ & & \vdots & & \\ 1 & m & m^2 & \cdots & m^m \end{array}\right], \quad \mathcal{Y}(t) := \left[\begin{array}{c} y(t)\\ y(t+h)\\ \vdots\\ y(t+mh)\end{array}\right], \tag{3.20}$$

$$H_m(h) = \ diag\{1, h, \frac{h^2}{2!}, \cdots, \frac{h^m}{m!}\}.$$

The control period T is defined to be

$$T := \begin{cases} mh & q = 0, \\ (q+2)mh & q \geq 1, \end{cases}$$

where $q \in \mathbb{N}$ is the order of the polynomial $\hat{f}_\varepsilon(g)$. Denoted the estimated ideal control signal by $\hat{u}^o(t)$ and a scaling factor $\rho > 0$, the controller in [1] is defined to be:

Controller: The controller is defined via five parts for $k \in \mathbb{Z}^+$.

(i) For $t \in [kT, kT + mh)$, set

$$\begin{aligned} u(t) &= \hat{u}^o(kT), \\ \hat{\phi}_0(kT) &:= \begin{bmatrix} \bar{f}_2 & -1 \end{bmatrix} H_m(h)^{-1} S_m^{-1} \mathcal{Y}(kT) + \begin{bmatrix} k_1 & k_2 \end{bmatrix} \begin{bmatrix} \bar{x}_m(kT) \\ \bar{u}_m(kT) \end{bmatrix}. \end{aligned} \tag{3.21}$$

(ii) If $q > 1$ and $t \in [kT + mh, kT + 2mh)$, set

$$\begin{aligned} u(t) &= \hat{u}^o(kT) + \rho\hat{\phi}_0(kT), \\ \hat{\phi}_1(kT) &:= \tfrac{1}{\rho} \begin{bmatrix} 0 & \cdots & 0 & 1 \end{bmatrix} H_m(h)^{-1} S_m^{-1} [\mathcal{Y}(kT + mh) - \mathcal{Y}(kT)]. \end{aligned} \tag{3.22}$$

(iii) If $q > 1$ and $t \in [kT + imh, kT + (i+1)mh)$, $i = 2, \ldots, q$, set

$$\begin{aligned} u(t) &= \hat{u}^o(kT) + \rho\hat{\phi}_{i-1}(kT) - \rho\hat{\phi}_{i-2}(kT), \\ \hat{\phi}_i(kT) &:= \hat{\phi}_{i-1}(kT) + \tfrac{1}{\rho} \begin{bmatrix} 0 & \cdots & 0 & 1 \end{bmatrix} H_m(h)^{-1} S_m^{-1} [\mathcal{Y}(kT + imh) - \mathcal{Y}(kT)]. \end{aligned} \tag{3.23}$$

(iv) If $q > 1$ and $t \in [kT + (q+1)mh, kT + (q+2)mh) = [kT + (q+1)mh, (k+1)T)$, set

$$u(t) = \hat{u}^o(kT) - \rho\hat{\phi}_{q-1}(kT). \tag{3.24}$$

(v) In all cases, set

$$\hat{u}^o[(k+1)T] = \hat{u}^o(kT) + \sum_{i=0}^{q} c_i \hat{\phi}_i(kT), \qquad \hat{u}^o[0] = \hat{u}_0^o. \tag{3.25}$$

In [1], it is shown that if a reasonable condition $\varepsilon < 1$ is imposed, then **the controller**

should do a good job of estimating the ideal control law. In addition, the following remark shows that the estimation can be extremely simple.

Remark 2. *(Remark 3 in [1]) If every element of $\mathcal{G}$ is positive, then there exist positive $\underline{g}, \bar{g} \in \mathbb{R}$ satisfying $\mathcal{G} \subset [\underline{g}, \bar{g}]$. If we set $\hat{f}_\varepsilon$ to be constant and of value $\hat{f}_\varepsilon(g) = \frac{1}{2\bar{g}}$, then it is easy to confirm that*

$$|1 - g\hat{f}_\varepsilon(g)| \leq 1 - \frac{\underline{g}}{2\bar{g}} < 1, \quad g \in \mathcal{G}.$$

This means that we can use a zero-th order polynomial to get $\varepsilon < 1$, and if it was used in the afore-mentioned control law then there is no probing[3].

In addition to **Remark 2**, when there is not probing, $q = 0$ and $\hat{f}_\varepsilon(q) = c_0$. Hence, to ensure closed-loop stability, we need to satisfy $|1 - gc_0| < 1$. In other words, for $g \in [\underline{g}, \bar{g}]$, the good range of c_0 is $(0, \frac{2}{\bar{g}})$.

As the main result, **Theorem 1** from [1] shows some desirable features of the controller:

Theorem 1. For every $\delta > 0$ and $\lambda \in (\max\{\lambda_0, \lambda_m\}, 0)$ there exists a controller of the form (3.4), (3.5), and (3.7) with the following properties:

(i) the controller exponentially stabilizes $\bar{\mathcal{P}}$, and

(ii) for every $\bar{\theta} \in \bar{\mathcal{P}}$, $\bar{x}_0 \in R^{n+n_m+1}$, and $u_m \in PC_\infty$, when $t_0 = k_0 = 0$ the closed-loop system satisfies

$$|y(t) - y_m(t) - \bar{C}\Phi_{cl}(t, 0)\bar{x}(0)| \leq \delta e^{\lambda t}(\|\bar{x}_0\| + |\hat{u}_0^0|) + \delta\|u_m\|_\infty, \quad t \geq 0.$$

Remark 3. *It is important to point out that this controller is linear (time-varying) and exponentially stabilizes the plant. Since the controller is linear (time-varying) and exponentially stabilizes the plant, one can prove that this controller is able to tolerate sufficiently small unmodeled dynamics.*

[3]The concept of probing is used in both [1] and [3]. Probing refers to the test signals that the controller uses to 'probe' the plant during a control period. The controller collects information of how the plant respond to the probing signals and then decide the control signal. For the controller from [1], probing signals refers to equation (3.22)-(3.24).

3.4 Examples

Since most features can be clearly illustrated with a first order plant, the examples from [1] focus on such a system[4]. To this end, consider the first order time-varying plant

$$\dot{y}(t) = a(t)y(t) + g(t)u(t). \tag{3.26}$$

The set of *uncertainty* is chosen to be

$$\bar{\mathcal{P}}(n = 1, m = 1, \bar{\Gamma}, \bar{\mu}_1 = 1, \bar{T}_0 = 5, \underline{g}, \gamma_0 = 1, \lambda_0 = -5),$$

where $\bar{\Gamma}$ and $\underline{g}$ are different for each example. The *reference model* is

$$\dot{\bar{y}}_m = -\bar{y}_m + \bar{u}_m$$

while the reference model *anti-aliasing filter* is chosen to be

$$\dot{\bar{u}}_m = -50\bar{u}_m + 50u_m.$$

In addition, we choose the probing scaling parameter $\rho = 1$ and set u_m to be a square wave

$$u_m(t) = \text{sign}\left(\cos(\frac{2\pi t}{15})\right).$$

Example 1 in [1] simulates the case where the sign of the high frequency gain is known. It is considered that

$$\bar{\Gamma} = \{\begin{bmatrix} a \\ g \end{bmatrix} \in \mathbb{R}^2 : a \in [-1, 1], g \in [0.5, 1.5]\}, \ \underline{g} = 0.5. \tag{3.27}$$

Figure 3.2 shows the simulations with plant parameters $a(t) = \cos(t/2)$ and $g(t) = [1 + 0.5\sin(t/4)]$ and initial conditions $y_0 = 3$, $\bar{u}_{m_0} = 0$. In this simulation, the sampling period h is chosen to be 0.01 second. In addition, random noise of maximum magnitude of 0.01 is injected at the output measurement at $t = 66$ seconds. As we can see, the redesigned LPC presented in [1] gives good performance and a somewhat smooth control signal. More importantly, it **has excellent noise rejection** - the effect of noise on the plant output is almost invisible; the effect of noise on the control input is minimal.

[4]For most of the following simulations, note that it is often comparing the responses of the original LPC (controller from [3]) and the redesigned LPC (controller from [1]). However our interest is the response of the redesigned LPC.

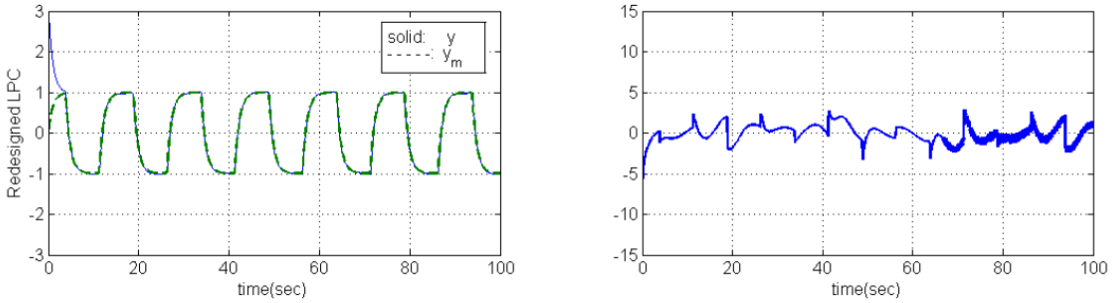

Figure 3.2: The plant output and control signal with a and g varying with time [1]

On the other hand, **Example 2** in [1] simulates the case where the sign of the high frequency gain is unknown. Here we have:

$$\bar{\Gamma} = \{ \begin{bmatrix} a \\ g \end{bmatrix} \in \mathbb{R}^2 : a \in [-1, 1], g^2 \in [1, 1.4] \}, \ \underline{g} = 1. \tag{3.28}$$

Figure 3.3 shows the simulations with plant parameters $a(t) = \cos(t/2)$ and $g(t) = [1.2 + 0.2\sin(t/2)] \times \text{sign}[\cos(t/4)]$ and initial conditions $y_0 = 3$, $\bar{u}_{m_0} = 0$. The sampling period h is chosen to be 0.01 second. The random noise signal of maximum magnitude of 0.01 is injected at the output measurement at $t = 66$ seconds. We can see, the redesigned LPC presented in [1] gives good performance and a somewhat smooth control signal. However, the noise rejection is not as good as the previous case - the effect of noise on the plant output is visible; the control signal looks noisy.

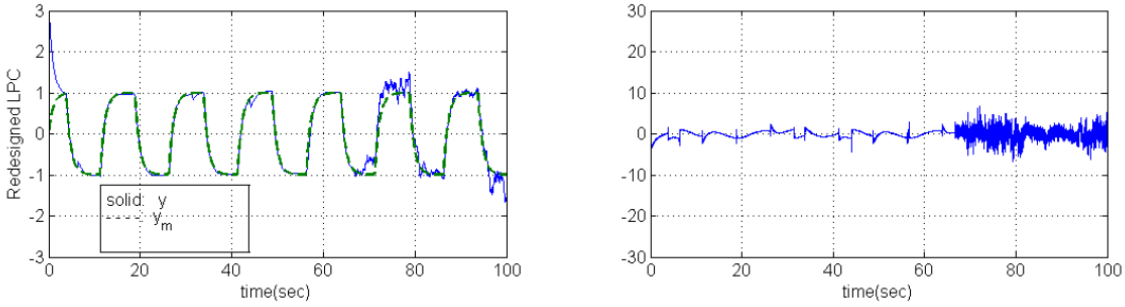

Figure 3.3: The plant output and control signal with a and g varying with time [1]

3.5 Noise Behavior

The previous simulations examined the tracking performance and noise behavior for one sampling period. Interestingly, for the case where the sign of the high frequency gain is known, noise has a small impact on the system. When the noise is small in size, it almost has no effect on the output. Hence, it is clearly of interest to carefully examine the tradeoff between performance and noise rejections as a function of the sampling period h. This has also been looked at in [1]. In the existence of noise, let $y_n(t) := y(t) + n(t)$ denote the measured output and T_{ny_n} denote the corresponding map from $n \to y_n$.[5] Define

$$\|T_{ny_n}\| := \sup\{\frac{\|T_{ny_n} n\|_\infty}{\|n\|_\infty} : n \in PC_\infty, 0 < \|n\|_\infty < \infty\},$$

to be the induced noise gain from the noise to the measured output. First, we are going to look at the case where the sign of the high frequency gain is known. Consider the case of Example 1. Figure 3.4 plots $\|T_{ny_n}\|$ as a function of the sampling period. We observe that

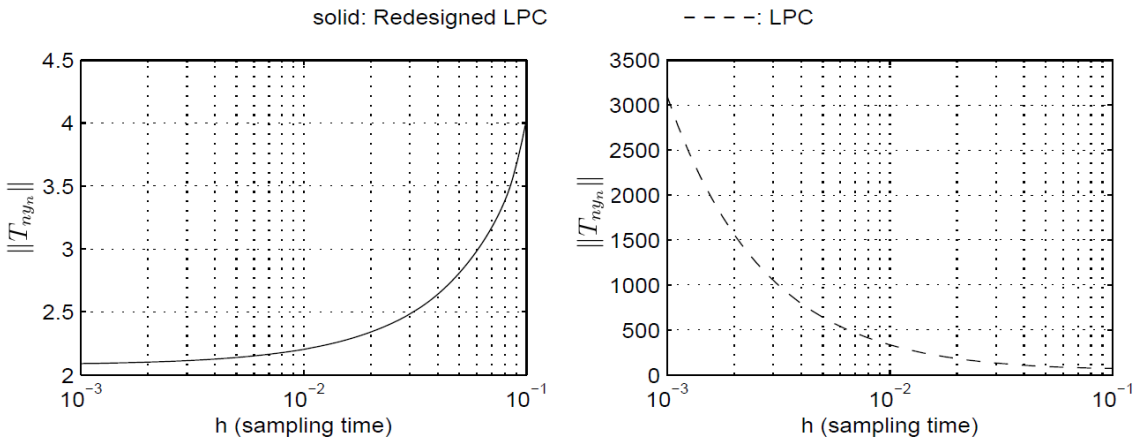

Figure 3.4: $\|n \to y_n\|$ for the case where the high frequency gain is known

as the sampling period decreases, the induced noise gain tends toward a constant value around 2. Generally speaking, as the sampling period gets smaller, the high frequency component of the noise is amplified, which makes the estimation inaccurate and therefore

[5] In [1], to investigate the induced noise gain, the map $n \to e$ has been looked at instead of $n \to y_n$. However, the gain of $\|n \to e\|$ and $\|n \to y_n\|$ are exactly the same.

distorts the control signal. This behavior is observed in the original LPC but not the redesigned LPC. Indeed, this nice behavior on the induced noise gain of the redesigned LPC is desirable.

To demonstrate this behavior more clearly, another simulation is carried out with using different sampling periods. For the following simulation, we choose

$$\bar{\Gamma} = \{ \begin{bmatrix} a \\ g \end{bmatrix} \in \mathbb{R}^2 : a \in [-1, 1], g \in [0.5, 1.5] \}, \ \underline{g} = 0.5. \tag{3.29}$$

Figure 3.5 shows the simulations with plant parameters $a(t) = \cos(t)$ and $g(t) = [1 + 0.5\sin(t/2)]$ and initial conditions $y_0 = 3$, $\bar{u}_{m_0} = 0$. The sampling period h is chosen to be 0.1s, 0.01s, and 0.001s respectively. To clearly demonstrate the noise behavior, we choose large random noise signals with maximum magnitude of 1 (100 times bigger than the ones in Example 1). In this simulation, we observe that with large size random noise, the plant

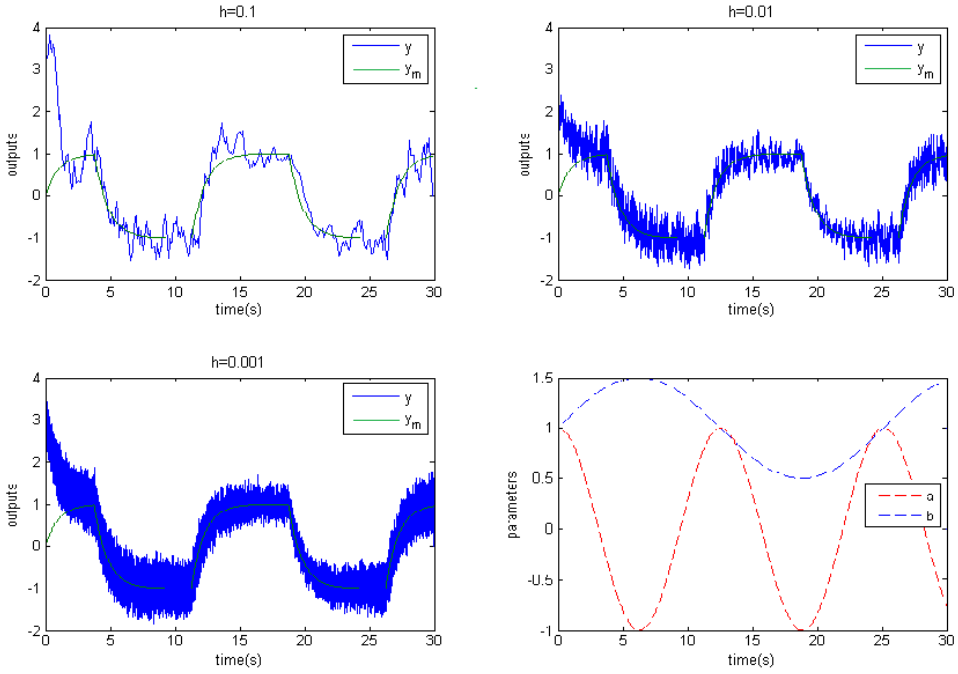

Figure 3.5: The plant outputs simulated with different sampling period; parameter a and g are time-varying.

output still tracks the reference output well. In addition, the output plots appears to superimpose the noise on the 'noiseless' output.

Now, we are going to look at the case where the sign of the high frequency gain is unknown. For the case of Example 2, Figure 3.6 plots $\|T_{ny_n}\|$ as a function of the sampling period h. From this simulation, we observe that the noise gain of the redesigned LPC

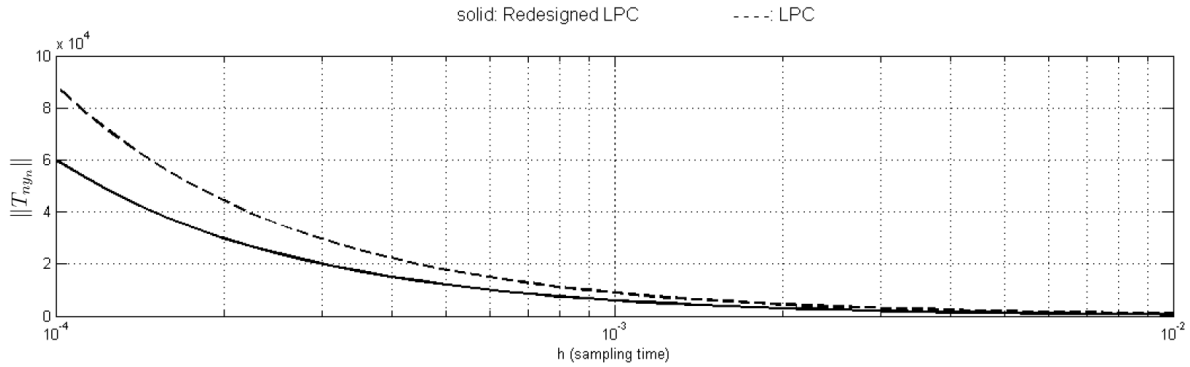

Figure 3.6: $\|n \to y_n\|$ for the case where the high frequency gain is unknown

amplifies with decreasing sampling period. This is an undesirable feature of the controller. For faster convergence and a better tracking, the redesigned LPC requires a faster sampling rate. If the sign of the high frequency gain is unknown, smaller sampling period implies worse noise rejection. Clearly, tracking performance and noise rejection are the tradeoffs.

3.6 Goal

In the previous section, we examined the noise behavior with different sampling periods. For the case where the sign of the high frequency gain is unknown, as the sampling period h decreases, T_{ny_n} increases. On the other hand, if we assume that the sign of the high frequency gain is known, the system has good noise rejection even when the sampling period is small. Hence, in the rest of the paper, we will **assume that the sign of the high frequency gain is known.** In particular, we assume[6]

[6]We implicitly assumed that the sign of the high frequency gain is positive, for if it is negative, we can absorb it into u.

- *Assumption* 7: (Regularity of g) There exists a positive constant $\bar{g}$ so that $g(t) \in [\underline{g}, \bar{g}]$ for all $t \geq 0$.

Figure 3.4 indicates that as $h \to 0$, the induced noise gain $\|T_{ny_n}\|$ approaches a constant number around 2. However, there are still a few questions remaining:

1. What is the constant? Is it exactly at 2.0?
2. The simulation from (3.4) examines only the size of the induced noise gain for one particular first order plant. Can this result be applied to other types of plants? (i.e. other first order time-varying plants, relative degree one plants, or second order plants?)
3. Can we change the controller in such a way that the induced noise gain can be reduced? How much can we improve?

The assumptions in [1] allow infrequent jumps on the plant parameters. In this thesis, to simplify the proof, we impose an additional assumption:

- *Assumption* 8: $\bar{\theta}(t)$ is absolutely continuous for all $t \geq 0$.

Since we are interested in the set of plants with plant uncertainties of the form (3.13) and assuming that $\bar{\theta}(t)$ is absolutely continuous, we update the set of plant uncertainty to be of the form

$$\bar{\mathcal{P}}_{ac}(n, m, \bar{\Gamma}, \bar{\mu}_1, \bar{T}_0, \underline{g}, \gamma_0, \lambda_0). \tag{3.30}$$

Next, we will look at some different notations. Since our interest is the effect of noise on the plant output, let T_{ny} denote the map from $n \to y$ and define

$$\|T_{ny}\| := \sup\{\frac{\|T_{ny}n\|_\infty}{\|n\|_\infty} : n \in PC_\infty,\ 0 < \|n\|_\infty < \infty\}. \tag{3.31}$$

It is easy to see that

$$T_{ny_n} = T_{ny} + 1.$$

Since T_{ny} is strictly causal, it follows that

$$\|T_{ny_n}\| = \|T_{ny}\| + 1.$$

Hence, if the simulation of Figure 3.4 indicates that as $h \to 0$,

$$\|T_{ny_n}\| \to 2,$$

then we should have

$$\|T_{ny}\| \to 1.$$

In the rest of the thesis, we will look at $\|T_{ny}\|$ instead of $\|T_{ny_n}\|$.

3.7 Controller for the relative degree one case

In this thesis, all the plants under consideration are relative degree one ($m = 1$) and has known sign of the high frequency gain. Here, we will first simplify and formulate the controller to the cases we consider. According to **Remark 1**, we can use a zero-th order polynomial to get $\varepsilon < 1$, and if it it used in the afore-mentioned control law, then no probing is needed (i.e. $q = 1$). With this information, the complexity of the controller is greatly simplified. For $k \in \mathbb{Z}^+$, the controller can be reduced to:

$$\begin{array}{rcl} \hat{\phi}_0(kT) & := & \left[\begin{array}{cc} \bar{f}_2 & -1 \end{array}\right] H_1(h)^{-1} S_1^{-1} \mathcal{Y}(kT) + \left[\begin{array}{cc} k_1 & k_2 \end{array}\right] \left[\begin{array}{c} \bar{x}_m(kT) \\ \bar{u}_m(kT) \end{array}\right], \\ \hat{u}^o[(k+1)T] & = & \hat{u}^o(kT) + c_0 \hat{\phi}_0(kT), \qquad \hat{u}^o(0) = \hat{u}_0^o, \\ u(t) & = & \hat{u}^0(kT). \end{array} \tag{3.32}$$

In the presence of noise, the measurement of system output $y(kT)$ is distorted and affects the control signal. Here, denote the group of noisy outputs as

$$\mathcal{Y}_n(kT) := \left[\begin{array}{c} y(kT) + n(kT) \\ y(kT+h) + n(kT+h) \end{array}\right].$$

Thus, when noise is considered, $\mathcal{Y}_n$ should be used instead of $\mathcal{Y}$. From (3.32), notice that the reference signals $u_m(kT)$ and $x_m(kT)$ are linearly independent from the noise $n(kT)$. If one's interest is to know the system noise gain, the effect of u_m and x_m can be neglected. Hence, set $u_m = x_m = 0$. Combining the above information and substituting the values of S_m and $H_m(h)$, the controller can be expressed as:

$$\begin{array}{rcl} \hat{\phi}_0(kT) & = & \left[\begin{array}{cc} \bar{f}_2 & -1 \end{array}\right] \left[\begin{array}{cc} 1 & 0 \\ 0 & T \end{array}\right]^{-1} \left[\begin{array}{cc} 1 & 0 \\ 1 & 1 \end{array}\right]^{-1} \left[\begin{array}{c} y_n(kT) \\ y_n[(k+1)T] \end{array}\right], \\ u[(k+1)T] & = & u(kT) + c_0 \hat{\phi}_0(kT). \end{array} \tag{3.33}$$

Chapter 4

Fixed parameter case

In this chapter, we analyze the induced noise gain with the simplest setup. Here, a first order LTI plant is considered. In particular, we assume the set of plant uncertainty to be

$$\bar{\mathcal{P}}_{ac}(n=1, m=1, \bar{\Gamma}, \bar{\mu}_1 = 0, \underline{g}, \gamma_0, \lambda_0),$$

and the plant is parameterized by $\bar{\theta}(t) = \begin{bmatrix} \beta_0(t) \\ g(t) \end{bmatrix}$. As stated earlier, the objective is to find the maximum induced noise gain when the plant has relative degree one and the sign of the high frequency gain is known. Specifically, the goal is to obtain a closed form expression of the induced noise gain as $h \to 0^+$. The simulation from [1] shows that, for a particular example, the maximum induced noise gain goes to a constant value as the sampling period $h \to 0^+$. This chapter uses a theoretical approach to obtain a closed form expression of the maximum induced noise gain. In addition, based on the result, recommendations are given on the selection of the estimation parameter c_0 to ensure a small noise gain when the sampling period is small.

4.1 LTI system

For all the plants that have relative degree one, the first order LTI plant is the simplest. In this chapter, we are going to consider such a system. In addition, we assume that the sign of the high frequency gain is known. As we are going to see, when a first order linear time invariant plant with known sign of the high frequency gain is considered, using the controller provided in [1], the closed-loop system is linear time invariant.

4.1.1 First order plant

For $\begin{bmatrix} a \\ g \end{bmatrix} \in \bar{\Gamma}$, consider the first order LTI plant[1]

$$\dot{y}(t) = ay(t) + gu(t). \tag{4.1}$$

With the control period $T > 0$, since the plant parameters are fixed and the control signal $u(t)$ is piecewise constant on the interval $[kT, (k+1)T)$, the solution of (4.1) is

$$y[(k+1)T] = e^{aT}y(kT) + \frac{e^{aT}-1}{a}gu(kT). \tag{4.2}$$

Note that the above LTI plant is strictly proper and has relative degree one. Combining (3.33) and (4.2), it is not hard to recognize that the closed-loop system is LTI. The control signal is updated at the end of every control period and fed into the plant.

4.2 State Space Representation

To carry out the analysis, we are going to express the system with a state space representation. Here, the controller and the plant are treated as two subsystems that are connected in series and feedback. We first find state-space representation for each 'subsystem'. Then, we connect the two subsystems. After some algebraic manipulations, a state-space representation is obtained with taking the noise as the input of the system.

4.2.1 State Space Representation of the Controller

It follows from (3.33) that

$$u[(k+1)T] = u(kT) + c_0(\frac{1}{T} + \bar{f}_2)y_n(kT) + c_0(-\frac{1}{T})y_n[(k+1)T], \qquad k \geq 0. \tag{4.3}$$

Using the shifting theorem and expressing the above equation in the delay operator form, we have

$$u(kT) = u[(k-1)T] + c_0(\frac{1}{T} + \bar{f}_2)y_n[(k-1)T] + c_0(-\frac{1}{T})y_n(kT), \qquad k \geq 1. \tag{4.4}$$

[1]Instead of using $\bar{\theta} = \begin{bmatrix} \beta_0 \\ g \end{bmatrix}$, we use $\bar{\theta} = \begin{bmatrix} a \\ g \end{bmatrix}$ to embrace the natural notation of the first order LTI plant $\dot{y}(t) = ay(t) + gu(t)$.

Taking the $\mathcal{Z}$-transform of (4.4) and considering the initial conditions, we have:

$$\begin{aligned} \mathcal{U}[z] &= \tfrac{\mathcal{U}[z]}{z} + u(-1) + c_0(\tfrac{1}{T} + \bar{f}_2)(\tfrac{Y_N[z]}{z} + y_n(-1)) + c_0(-\tfrac{1}{T})Y_N[z], \\ \tfrac{z-1}{z}\,\mathcal{U}[z] &= \Big[c_0(\tfrac{1}{T} + \bar{f}_2)\tfrac{1}{z} + c_0(-\tfrac{1}{T})\Big]Y_N[z] + c_0(\tfrac{1}{T} + \bar{f}_2)y_n(-1) + u(-1), \end{aligned}$$

so

$$\mathcal{U}[z] = \underbrace{\frac{1}{z-1}\Big[c_0(\frac{1}{T} + \bar{f}_2) - \frac{c_0}{T}z\Big]Y_N[z]}_{\text{zero state response}} + \underbrace{\frac{z}{z-1}\Big[c_0(\frac{1}{T} + \bar{f}_2)y_n(-1) + u(-1)\Big]}_{\text{zero input response}}. \tag{4.5}$$

In our controller, the initial estimated input $\hat{u}^o(0)$ will be set to zero. Hence, we have $u(0) = \hat{u}^o(0) = 0$. Since we are looking at the induced noise gain from $n \to y$, then $y(k) = u(k) = n(k) = 0$ for all $k < 0$. Since the plant is strictly proper, we also have $y(0) = 0$. Equation (4.5) separates the system response into the zero state response and the zero input response. First, take a look at the zero state response. We have

$$\begin{aligned} \frac{\mathcal{U}[z]}{Y_N[z]} &= \frac{c_0(\frac{1}{T} + \bar{f}_2) - z(\frac{c_0}{T})}{z-1} \\ &= \frac{c_0(\frac{1}{T} + \bar{f}_2) - (z-1)\frac{c_0}{T} - \frac{c_0}{T}}{z-1} \\ &= \frac{c_0(\frac{1}{T} + \bar{f}_2 - \frac{1}{T})}{z-1} - \frac{c_0}{T} \\ &= c_0\bar{f}_2\frac{1}{z-1} - \frac{c_0}{T}. \end{aligned} \tag{4.6}$$

A natural choice of the state space representation (4.6) is:

$$\begin{aligned} x_1[(k+1)T] &= A_c x_1(kT) + B_c y_n(kT), \\ u(kT) &= C_c x_1(kT) + D_c y_n(kT), \end{aligned} \tag{4.7}$$

with $A_c = 1$, $B_c = 1$, $C_c = c_0\bar{f}_2$, and $D_c = -\frac{c_0}{T}$. In (4.7), the input is the plant output with noise. The output is the control signal $u(kT)$.

To find the initial state value, take the output equation from (4.7) and then substitute $k = 0$, so that

$$u(0) = c_0\bar{f}_2 x_1(0) - \frac{c_0}{T}y_n(0) = 0,$$

and

$$x_1(0) = \frac{1}{\bar{f}_2 T} y_n(0) = \frac{1}{\bar{f}_2 T} n(0).$$

Analyzing the system behavior using the above is complicated since $n(0)$ sets up an initial condition on the LTI controller model, which is unusual and conceptually difficult. To simplify the analysis, we will instead analyze the case in which $n(0) = 0$, thus avoiding this problem. Since the closed-loop system is time invariant, we can use the fact that the induced gain of the map from $n \to y$ is the same even though we impose this constraint.

4.2.2 State Space Representation of the Plant

Based on (4.2), a natural choice of the state space representation of the plant is:

$$\begin{aligned} x_2[(k+1)T] &= A_p x_2(kT) + B_p u(kT), \\ y(kT) &= C_p x_2(kT) + D_p u(kT), \end{aligned} \tag{4.8}$$

with $A_p = e^{aT}$, $B_p = \frac{e^{aT}-1}{a} g$, $C_p = 1$, and $D_p = 0$. From the output equation, it is observed that $y(kT) = x_2(kT)$. Thus, $x_2(0) = y(0)$. Hence, to find the induced noise gain, we can set the initial condition to be zero (i.e. $y(0) = x_2(0) = 0$).

4.2.3 System State Space Representation

Combining the controller (4.7) and the plant (4.8), yields

$$\begin{aligned} \begin{pmatrix} x_1[(k+1)T] \\ x_2[(k+1)T] \end{pmatrix} &= \begin{bmatrix} A_c & 0 \\ B_p C_c & A_p \end{bmatrix} \begin{pmatrix} x_1(kT) \\ x_2(kT) \end{pmatrix} + \begin{bmatrix} B_c \\ B_p D_c \end{bmatrix} y_n(kT), \quad \begin{pmatrix} x_1(0) \\ x_2(0) \end{pmatrix} = 0, \\ y(kT) &= \begin{bmatrix} D_p C_c & C_p \end{bmatrix} \begin{pmatrix} x_1(kT) \\ x_2(kT) \end{pmatrix} + \begin{bmatrix} D_p D_c \end{bmatrix} y_n(kT). \end{aligned}$$

Substituting values of (A_1, B_1, C_1, D_1) and (A_2, B_2, C_2, D_2) obtained earlier, we have

$$\begin{aligned} \begin{pmatrix} x_1[(k+1)T] \\ x_2[(k+1)T] \end{pmatrix} &= \begin{bmatrix} 1 & 0 \\ \frac{e^{aT}-1}{a} g c_0 \bar{f}_2 & e^{aT} \end{bmatrix} \begin{pmatrix} x_1(kT) \\ x_2(kT) \end{pmatrix} + \begin{bmatrix} 1 \\ -\frac{e^{aT}-1}{a} g \frac{c_0}{T} \end{bmatrix} (y(kT) + n(kT)), \\ y(kT) &= \begin{bmatrix} 0 & 1 \end{bmatrix} \begin{pmatrix} x_1(kT) \\ x_2(kT) \end{pmatrix}. \end{aligned}$$

Since $x_2(kT) = y(kT)$, we then have

$$\begin{array}{rcl} \begin{pmatrix} x_1[(k+1)T] \\ x_2[(k+1)T] \end{pmatrix} & = & \begin{bmatrix} 1 & 1 \\ (e^{aT}-1)\frac{gc_0\bar{f}_2}{a} & e^{aT}-(e^{aT}-1)\frac{gc_0}{aT} \end{bmatrix} \begin{pmatrix} x_1(kT) \\ x_2(kT) \end{pmatrix} + \begin{bmatrix} 1 \\ -(e^{aT}-1)\frac{gc_0}{aT} \end{bmatrix} n(kT), \\ y(kT) & = & \begin{bmatrix} 0 & 1 \end{bmatrix} \begin{pmatrix} x_1(kT) \\ x_2(kT) \end{pmatrix}. \end{array}$$

Finally, the **closed-loop state space equations** with noise being the only input of the system can be written as

$$\begin{array}{rcl} x[(k+1)T] & = & A_{cl}x(kT) + B_{cl}n(kT), \quad x(0) = 0, \\ y(kT) & = & C_{cl}x(kT) + D_{cl}n(kT), \end{array} \tag{4.9}$$

with

$$\begin{array}{rcl} A_{cl} & = & \begin{bmatrix} 1 & 1 \\ \left(e^{aT}-1\right)\frac{gc_0\bar{f}_2}{a} & e^{aT}-\left(e^{aT}-1\right)\frac{gc_0}{aT} \end{bmatrix}, \\ B_{cl} & = & \begin{bmatrix} 1 \\ -\left(e^{aT}-1\right)\frac{gc_0}{aT} \end{bmatrix}, \\ C_{cl} & = & \begin{bmatrix} 0 & 1 \end{bmatrix}, \\ D_{cl} & = & 0. \end{array}$$

4.3 The Diagonalized System

In the previous section, a system state space expression is obtained for first order plant with fixed-parameters. For a linear time-invariant system, the eigenvalues of A_{cl} play a key role on the stability of system (4.9). In the later sections, it is shown that the induced noise gain depends on the eigenvalues of A_{cl}. In this section, the goal is to diagonalize A_{cl} and find the similarity transformation.

4.3.1 Using Order Notation

Since the goal is to find noise gain as $T \to 0^+$, high order terms corresponding to the sampling period T can be neglected. Using the Taylor Series with order notation, we have:

1. $e^{aT} = 1 + aT + \mathcal{O}(T^2)$,
2. $\frac{\left(e^{aT}-1\right)}{aT} = \frac{\left[aT + \frac{(aT)^2}{2!} + \mathcal{O}\left(T^3\right)\right]}{aT} = 1 + \frac{\mathrm{aT}}{2} + \mathcal{O}(T^2)$.

Applying the above order notations to the closed loop system, the state matrices of (4.9) can be written as:

$$A_{cl} = \begin{bmatrix} 1 & 1 \\ gc_0\bar{f}_2T + \ \mathcal{O}(T^2) & 1 - c_0g + aT(1 - \frac{gc_0}{2}) + \mathcal{O}(T^2) \end{bmatrix},$$

$$B_{cl} = \begin{bmatrix} 1 \\ -gc_0 + \mathcal{O}(T) \end{bmatrix},\ C_{cl} = \begin{bmatrix} 0 & 1 \end{bmatrix},\ D_{cl} = 0.$$

4.3.2 Block-Diagonalization

In [2], a simple transformation is presented for time-invariant systems. This transformation diagonalizes the state matrix. In particular, for systems with one fast and one slow subsystems, this method is useful to separate the "slow" and "fast" eigenvalues of the subsystems. In our case, the plant acts "slowly" and the controller responds "rapidly". Using this diagonalization method, we can easily analyze how each eigenvalue affects the system output.

Step 1 - Upper triangular form

The first step of this transformation is to transform the state matrix A_{cl} into an upper triangular form. Denote

$$A_{cl} := \begin{bmatrix} A_{11} & A_{12} \\ A_{21} & A_{22} \end{bmatrix}.$$

With $L \in \mathbb{R}$, consider the following transformation

$$\begin{bmatrix} 1 & 0 \\ L & 1 \end{bmatrix} A_{cl} \begin{bmatrix} 1 & 0 \\ -L & 1 \end{bmatrix} = \begin{bmatrix} A_{11} - A_{12}L & A_{12} \\ LA_{11} + A_{21} - LA_{12}L - A_{22}L & LA_{12} + A_{22} \end{bmatrix}. \tag{4.10}$$

The goal here is to make the matrix into a upper triangle form. Thus, L is the real root of $LA_{11} + A_{21} - LA_{12}L - A_{22}L = 0$. Hence,

$$L\left(gc_0 - a\left(1 - \frac{gc_0}{2}\right)T + \mathcal{O}\left(T^2\right)\right) + gc_0\bar{f}_2T + \ \mathcal{O}(T^2) - L^2 = 0,$$

$$L^2 + \left(-gc_0 + a\left(1 - \frac{gc_0}{2}\right)T + \mathcal{O}\left(T^2\right)\right)L - gc_0\bar{f}_2T + \ \mathcal{O}\left(T^2\right) = 0. \tag{4.11}$$

Denote:

- $\bar{b} := -gc_0 + a\left(1 - \frac{gc_0}{2}\right)T + \mathcal{O}\left(T^2\right)$,
- $\bar{c} := -gc_0\bar{f}_2 T + \ \mathcal{O}\left(T^2\right)$,

then the solution of (4.11) is

$$\begin{aligned} L &= \frac{-\bar{b} \pm \sqrt{\bar{b}^2 - 4\bar{c}}}{2} \\ &= \frac{-\bar{b} \pm \left|\bar{b}\right| \sqrt{1 - \frac{4\bar{c}}{\bar{b}^2}}}{2}. \end{aligned}$$

Using the Taylor Series expansion, we can have,

$$\begin{aligned} \sqrt{1 - \tfrac{4\bar{c}}{\bar{b}^2}} &= 1 + \tfrac{1}{2}\left(-\tfrac{4\bar{c}}{\bar{b}^2}\right) - \tfrac{1}{8}\left(-\tfrac{4\bar{c}}{\bar{b}^2}\right)^2 + \cdots \\ &= 1 - \tfrac{2\bar{c}}{\bar{b}^2} - \tfrac{2\bar{c}^2}{\bar{b}^4} + \cdots, \end{aligned}$$

where

$$\begin{aligned} \tfrac{2\bar{c}}{\bar{b}^2} &= \frac{2\left(-gc_0\bar{f}_2 T + \ \mathcal{O}\left(T^2\right)\right)}{\left[-gc_0 + a\left(1 - \frac{gc_0}{2}\right)T + \mathcal{O}(T^2)\right]^2} \\ &= -\tfrac{2\bar{f}_2}{gc_0}T + \mathcal{O}(T^2), \end{aligned}$$

and

$$\frac{2\bar{c}^2}{\bar{b}^4} = \mathcal{O}(T^2).$$

Therefore, the two solutions of L are:

1. $L(T) = \frac{-\bar{b} + \left|\bar{b}\right|\sqrt{\bar{b}^2 - 4\bar{c}}}{2} = gc_0 - \left[a(1 - \frac{gc_0}{2}) + \bar{f}_2\right]T + \mathcal{O}(T^2) = \mathcal{O}(1)$,
2. $L(T) = \frac{-\bar{b} - \left|\bar{b}\right|\sqrt{\bar{b}^2 - 4\bar{c}}}{2} = -\bar{f}_2 T + \mathcal{O}(T^2)$.

Since this transformation should have a small impact on the diagonal terms of A_{cl}, we select the solution of $L(T)$ (or simply L) which is smaller for small T, namely

$$L = -\bar{f}_2 T + \mathcal{O}\left(T^2\right). \tag{4.12}$$

Substituting (4.12) into (4.10) yields

$$\begin{bmatrix} 1 & 0 \\ L & 1 \end{bmatrix} A_{cl} \begin{bmatrix} 1 & 0 \\ -L & 1 \end{bmatrix} = \begin{bmatrix} 1 + \bar{f}_2 T + \mathcal{O}\left(T^2\right) & 1 \\ 0 & 1 - gc_0 + \mathcal{O}\left(T\right) \end{bmatrix}.$$

Step 2 - Diagonalization

In this step, the upper triangular form is transformed to a diagonal form. Now, with $P \in \mathbb{R}$, consider the following transformation:

$$\begin{aligned} & \begin{bmatrix} 1 & P \\ 0 & 1 \end{bmatrix} \begin{bmatrix} 1 & 0 \\ L & 1 \end{bmatrix} A_{cl} \begin{bmatrix} 1 & 0 \\ -L & 1 \end{bmatrix} \begin{bmatrix} 1 & -P \\ 0 & 1 \end{bmatrix} \\ = & \begin{bmatrix} 1 & P \\ 0 & 1 \end{bmatrix} \begin{bmatrix} A_{11} - A_{12}L & A_{12} \\ 0 & LA_{12} + A_{22} \end{bmatrix} \begin{bmatrix} 1 & -P \\ 0 & 1 \end{bmatrix} \\ = & \begin{bmatrix} A_{11} - A_{12}L & (A_{11} - A_{12}L)(-P) + A_{12} + P(LA_{12} + A_{22}) \\ 0 & LA_{12} + A_{22} \end{bmatrix}. \end{aligned} \tag{4.13}$$

To make the matrix diagonal, P is the real root of $(A_{11} - A_{12}L)(-P) + A_{12} + P(LA_{12} + A_{22}) = 0$. Using values from A_{cl}, we have

$$\begin{aligned} (1 - L)(-P) + 1 + P(L + A_{22}) &= 0, \\ \implies P(-1 + 2L + A_{22}) &= -1, \\ \implies P &= \tfrac{1}{1-2L-A_{22}} \\ &= \tfrac{1}{1+2\bar{f}_2 T + \mathcal{O}(T^2) - (1 - gc_0 + \mathcal{O}(T))} \\ &= \tfrac{1}{gc_0 + \mathcal{O}(T)}. \end{aligned}$$

Thus,

$$P = \frac{1}{gc_0} + \mathcal{O}(T). \tag{4.14}$$

With L and P given by (4.12) and (4.14), and the transformation shown in (4.13), we are able to transform A_{cl} into a diagonal form. Let

$$\mathcal{T}^{-1} := \begin{bmatrix} 1 & P \\ 0 & 1 \end{bmatrix} \begin{bmatrix} 1 & 0 \\ L & 1 \end{bmatrix} \quad \text{and} \quad \mathcal{T} := \begin{bmatrix} 1 & 0 \\ -L & 1 \end{bmatrix} \begin{bmatrix} 1 & -P \\ 0 & 1 \end{bmatrix}.$$

Denote $\bar{A}_{cl} := \mathcal{T}^{-1} A_{cl} \mathcal{T}$, $\bar{B}_{cl} := \mathcal{T}^{-1} B_{cl}$, and $\bar{C}_{cl} := C_{cl} \mathcal{T}$. This yields

$$\begin{aligned} \bar{A}_{cl} =: \begin{bmatrix} \lambda_1 & 0 \\ 0 & \lambda_2 \end{bmatrix} &= \begin{bmatrix} 1 - L & 0 \\ 0 & L + A_{22} \end{bmatrix} \\ &= \begin{bmatrix} 1 + \bar{f}_2 T + \mathcal{O}(T^2) & 0 \\ 0 & 1 - gc_0 + \mathcal{O}(T) \end{bmatrix}, \end{aligned}$$

$$
\begin{aligned}
\bar{B}_{cl} \;=:\; \begin{bmatrix} \bar{B}_{cl_1} \\ \bar{B}_{cl_2} \end{bmatrix} &= \begin{bmatrix} 1+PL & P \\ L & 1 \end{bmatrix} \begin{bmatrix} 1 \\ -gc_0+\mathcal{O}(T) \end{bmatrix} \\
&= \begin{bmatrix} 1+PL+P(-gc_0+\mathcal{O}(T)) \\ L-gc_0+\mathcal{O}(T) \end{bmatrix} \\
&= \begin{bmatrix} 1+(\frac{1}{gc_0}+\mathcal{O}(T))(-\bar{f}_2T+\mathcal{O}\left(T^2\right))+(\frac{1}{gc_0}+\mathcal{O}(T))(-gc_0+\mathcal{O}(T)) \\ -\bar{f}_2T+\mathcal{O}(T^2)-gc_0+\mathcal{O}\left(T\right) \end{bmatrix} \\
&= \begin{bmatrix} \mathcal{O}(T) \\ -gc_0+\mathcal{O}(T) \end{bmatrix}, \\
\bar{C}_{cl} \;=:\; \begin{bmatrix} \bar{C}_{cl_1} & \bar{C}_{cl_2} \end{bmatrix} &= \begin{bmatrix} 0 & 1 \end{bmatrix} \begin{bmatrix} 1 & -P \\ -L & 1+PL \end{bmatrix} \\
&= \begin{bmatrix} -L & PL+1 \end{bmatrix} \\
&= \begin{bmatrix} \bar{f}_2T+\mathcal{O}\left(T^2\right) & 1+\frac{-\bar{f}_2}{gc_0}T+\mathcal{O}\left(T^2\right) \end{bmatrix} \\
&= \begin{bmatrix} \bar{f}_2T+\mathcal{O}\left(T^2\right) & 1+\mathcal{O}(T) \end{bmatrix}.
\end{aligned}
$$

From the above equations, observe that the first eigenvalue of $\bar{A}_{cl}$ is related to the reference model parameter a_m, since $\bar{f}_2$ is chosen so that $\bar{f}_2 \leq a_m$. On the other hand, the second eigenvalue $1-gc_0+\mathcal{O}(T)$ is characterized by the controller, and the size of the second eigenvalue depends on the controller parameter c_0.

4.4 Analyze the LTI system

In the previous sections, we found a discrete time state-space representation of the system. Using the afore-mentioned dicrete time state-space representation, we obtain information of the input/output at the sampling point. However, the induced noise gain should be computed using continuous signals (i.e. $y(t)$ and $n(t)$). For this reason, we will first look at the discrete time plant output (i.e. $y(kT)$). Then we will analyze the output between the sample points to get a full picture of the output $y(t)$.

4.4.1 Impulse response

For a LTI SISO discrete-time system, the infinity norm induced gain is equal to the one norm of the impulse response. In other words, with n being the input, y being the output,

and $h(j)$ for $j \in \mathbb{Z}^+$ being the impulse response, we have[2]

$$\sup\left\{\frac{\sup_{k\geq 0}|y(kT)|}{\sup_{k\geq 0}|n(kT)|} : 0 < \sup_{k\geq 0}|n(kT)| < \infty\right\} = \sum_{j=0}^{\infty}|h(j)|.$$

This is a well-known result and has been proved in [19]. For $i \in \mathbb{Z}^+$, the impulse response of the state-space model represented in (4.9) can be summarized as

$$h(i) = \begin{cases} D_{cl} & i = 0, \\ C_{cl}A_{cl}^{i-1}B_{cl} & i > 0. \end{cases} \tag{4.15}$$

Using the diagonalization method introduced in (4.13) yields

$$\begin{aligned} \textstyle\sum_{i=0}^{\infty}|h(i)| &= \textstyle\sum_{i=1}^{\infty}|h(i)| \\ &= \textstyle\sum_{i=1}^{\infty}\left|C_{cl}{A_{cl}}^{i-1}B_{cl}\right| \\ &= \textstyle\sum_{i=1}^{\infty}\left|\bar{C}_{cl}\bar{A}_{cl}^{i-1}\bar{B}_{cl}\right| \\ &= \textstyle\sum_{i=1}^{\infty}\left|\bar{C}_{cl_1}{\lambda_1}^{i-1}\bar{B}_{cl_1} + \bar{C}_{cl_2}{\lambda_2}^{i-1}\bar{B}_{cl_2}\right|, \end{aligned}$$

so

$$\sum_{i=0}^{\infty}|h(i)| \leq \sum_{i=1}^{\infty}\left|\bar{C}_{cl_1}{\lambda_1}^{i-1}\bar{B}_{cl_1}\right| + \sum_{i=1}^{\infty}\left|\bar{C}_{cl_2}{\lambda_2}^{i-1}\bar{B}_{cl_2}\right|,$$

It follows that[3]

$$\sup_{k\geq 0}|y(kT)| \leq \Big(\sum_{i=1}^{\infty}\left|\bar{C}_{cl_1}{\lambda_1}^{i-1}\bar{B}_{cl_1}\right| + \sum_{i=1}^{\infty}\left|\bar{C}_{cl_2}{\lambda_2}^{i-1}\bar{B}_{cl_2}\right|\Big)\|n\|_{\infty}. \tag{4.16}$$

4.4.2 Maximum induced noise gain

Now, we are going to analyze each part of (4.16) to find the maximum induced noise gain. As $T \to 0$, the first eigenvalue λ_1=$1 + \bar{f}_2T + \mathcal{O}(T^2)$ is a positive value close but less than 1. Substitute the matrix value obtained previously, we have:

$$\begin{aligned} \textstyle\sum_{i=1}^{\infty}\left|\bar{C}_{cl_1}{\lambda_1}^{i-1}\bar{B}_{cl_1}\right| &= \left|\left[\bar{f}_2T + \mathcal{O}(T^2)\right]\right|\left|\left[\tfrac{1}{-\bar{f}_2T+\mathcal{O}(T^2)}\right]\right||\mathcal{O}(T)| \\ &= \big(1 + \mathcal{O}(T)\big)|\mathcal{O}(T)| \\ &= \mathcal{O}(T). \end{aligned} \tag{4.17}$$

[2]In discrete time systems, we usually denote $\|y\|_{\infty} = \sup_{k\geq 0}|y(kT)|$. However, in this thesis, since our signals are in continuous time, we set $\|y\|_{\infty} = \sup_{t\geq 0}|y(t)|$. To avoid mixing continuous and discrete signals, we use $\sup_{k\geq 0}|y(kT)|$ to denote the infinity norm of discrete time signal $y(kT)$.

[3]Since $n \in PC_{\infty}$ is arbitrary and bounded, we can say that $\|n\|_{\infty} = \sup_{k\geq 0}|n(kT)| = \sup_{t\geq 0}|n(t)|$.

Hence, the first eigenvalue has only minor affect on the plant output.

On the other hand, the second eigenvalue $\lambda_2 = 1 - gc_0 + \mathcal{O}(T)$ has a magnitude strictly less than one, although λ_2 itself can be either positive and negative. Using the property of the sum of geometric series, we have:

a. If $\lambda_2 \geq 0$, then $\sum_{i=1}^{\infty} \left|{\lambda_2}^{i-1}\right| = \frac{1}{1-\lambda_2}$ and

$$\begin{aligned} \sum_{i=1}^{\infty} \left|\bar{C}_{cl_2} {\lambda_2}^{i-1} \bar{B}_{cl_2}\right| &= \left|\bar{C}_{cl_2}\right| \left|\sum_{i=1}^{\infty} \lambda_2^{i-1}\right| \left|\bar{B}_{cl_2}\right| \\ &= \left|[1+\mathcal{O}(T)]\left[\tfrac{-gc_0+O(T)}{gc_0+O(T)}\right]\right| \\ &= 1+\mathcal{O}(T). \end{aligned} \tag{4.18}$$

b. If $\lambda_2 < 0$, then $\sum_{i=1}^{\infty} \left|{\lambda_2}^{i-1}\right| = \frac{1}{1+\lambda_2}$ and

$$\begin{aligned} \sum_{i=1}^{\infty} \left|\bar{C}_{cl_2} {\lambda_2}^{i-1} \bar{B}_{cl_2}\right| &= \left|\bar{C}_{cl_2}\right| \left|\sum_{i=1}^{\infty} \lambda_2^{i-1}\right| \left|\bar{B}_{cl_2}\right| \\ &= \left|[1+\mathcal{O}(T)]\left[\tfrac{-gc_0+O(T)}{2-gc_0+\mathcal{O}(T)}\right]\right| \\ &= \left|\tfrac{gc_0}{2-gc_0}\right| + \mathcal{O}\left(T\right). \end{aligned} \tag{4.19}$$

From the above results, as $T \to 0^+$, the maximum noise gain is not dependent on plant parameter a. On the other hand, the selection of c_0 directly affects the noise gain. Combining the results in (4.17), (4.18), and (4.19) with (4.16), it is easy to check that

i. If $0 \leq \lambda_2 < 1$, then

$$\begin{aligned} \sup_{k\geq 0} |y(kT)| &\leq \left(\sum_{i=1}^{\infty} \left|\bar{C}_{cl_1} {\lambda_1}^{i-1} \bar{B}_{cl_1}\right| + \sum_{i=1}^{\infty} \left|\bar{C}_{cl_2} {\lambda_2}^{i-1} \bar{B}_{cl_2}\right|\right) \|n\|_{\infty} \\ &= \big(1+\mathcal{O}(T)\big)\|n\|_{\infty}. \end{aligned} \tag{4.20}$$

ii. If $-1 < \lambda_2 < 0$, then

$$\begin{aligned} \sup_{k\geq 0} |y(kT)| &\leq \left(\sum_{i=1}^{\infty} \left|\bar{C}_{cl_1} {\lambda_1}^{i-1} \bar{B}_{cl_1}\right| + \sum_{i=1}^{\infty} \left|\bar{C}_{cl_2} {\lambda_2}^{i-1} \bar{B}_{cl_2}\right|\right) \|n\|_{\infty} \\ &= \left(\left|\frac{gc_0}{2-gc_0}\right| + \mathcal{O}(T)\right)\|n\|_{\infty}. \end{aligned} \tag{4.21}$$

So far, we have examined the affect of noise on the plant output at the sample points. We see that the 'noisy plant output' is well behaved at the sample points. However, we still do not know the inter-sample behavior of the plant output. With a first order LTI plant, the answer is actually simple.

Claim 1. *If a and b are bounded fixed values, then for $k \in \mathbb{Z}^+$ and $t \in [kT, (k+1)T)$, the system:*

$$\begin{array}{rcl} y(t) & = & e^{at}y(kT) + \int_0^t e^{a\tau}bu(t-\tau)d\tau, \\ u(t) & = & u(kT), \end{array} \tag{4.22}$$

has the following property

$$|y(t)| \leq \max\{|y(kT)|, |y[(k+1)T]|\}.$$

Proof. Taking the derivative of the $y(t)$ equation and use the fact that $u(t)$ is constant in $[kT, (k+1)T)$, we have:

$$\begin{array}{rcl} \dot{y}(t) & = & ae^{at}y(kT) + e^{at}bu(kT) \\ & = & \underbrace{[ay(kT) + bu(kT)]}_{=:c}e^{at} \\ & = & ce^{at}. \end{array} \tag{4.23}$$

Hence, for $t \in [kT, (k+1)T)$, the sign of $\dot{y}(t)$ does not change. Therefore, we can directly conclude that

$$|y(t)| \leq \max\{|y(kT)|, |y[(k+1)T]|\}.$$

□

From the above, we see that the output is also well behaved between every sample points. Hence, the results of (4.20) and (4.21) can be extend to:

i. If $0 \leq \lambda_2 < 1$, then

$$\frac{\|y\|_\infty}{\|n\|_\infty} = 1 + \mathcal{O}(T), \tag{4.24}$$

ii. If $-1 < \lambda_2 < 0$, then

$$\frac{\|y\|_\infty}{\|n\|_\infty} = \left|\frac{gc_0}{2 - gc_0}\right| + \mathcal{O}(T). \tag{4.25}$$

Note that in the second case, $gc_0 > 1$ so $\left|\frac{gc_0}{2-gc_0}\right| > 1$. This means that when $0 \leq \lambda_2 < 1$, the induced noise gain is smaller. However, $\lambda_2 = 1 - gc_0 + \mathcal{O}(T)$ and $g \in [\underline{g}, \bar{g}] \subset (0, \infty)$. Hence, if we **choose** $c_0 \in (0, \frac{1}{\bar{g}})$**, then for small** T**, we will be guaranteed to have** $\lambda_2 \in [0, 1)$, so that (4.24) holds.

Proposition 1. *For a first order time-invariant plant of the form (4.1), for which the sign of the high frequency gain is known, using controller (3.21)-(3.25), the maximum induced noise gain is bounded. In particular, if the selection of* c_0 *satisfies* $c_0 \in (0, \frac{1}{\bar{g}})$*, then for every* $\delta > 0$*, there exists a* $\bar{T} > 0$ *such that for every* $T \in (0, \bar{T})$ *and* $\bar{\theta} \in \bar{\mathcal{P}}_{ac}(n = 1, m = 1, \bar{\Gamma}, \bar{\mu}_1 = 0, \underline{g}, \gamma_0, \lambda_0)$*, we have*

$$\|T_{ny}(\bar{\theta}, T)\| \leq 1 + \delta. \tag{4.26}$$

Proof. The proof follows from (4.24). □

Remark 4. *In [1], it is required that* $|1 - gc_0| \in (0, 1)$*. To ensure that this holds for all* $g \in [\underline{g}, \bar{g}]$*, we need to choose* $c_0 \in (0, \frac{2}{\bar{g}})$*. Here, we select* $c_0 \in (0, \frac{1}{\bar{g}})$ *which means that* $gc_0 \in (0, 1)$*. By sacrificing about half of the allowed range of* c_0*, we ensured a low noise gain - '*$1 + \mathcal{O}(T)$*'.*

4.5 Simulation Results

As a verification to the previous results, simulations are generated in this section. To begin, consider the following first order linear time-invariant plant

$$\dot{y}(t) = ay(t) + gu(t),$$

where a and g are the fixed plant parameters. The reference model is

$$\dot{\bar{y}}_m = -\bar{y}_m + \bar{u}_m, \tag{4.27}$$

so that $a_m = -1$ (stable) and $b_m = 1$. The modeled input u_m is set to be a square wave such that

$$u_m(t) = sign(cos(\frac{2\pi t}{15})). \tag{4.28}$$

The reference model anti-aliasing filter is chosen to be

$$\dot{\bar{u}}_m = -50\bar{u}_m + 50u_m. \tag{4.29}$$

With the above reference model setup, the modeled output goes in between ± 1. To provide good visibility to the behavior of the noise, we choose $||n||_\infty = 1$. Also, in all the following simulations, we choose $y(0) = 3$ and $u(0) = 0$ to be the initial conditions. In addition, in all cases, we choose $a = 1$ so that we have an unstable plant.

4.5.1 Example 1

When $gc_0 \in (0, 1)$, our result shows that the maximum induced noise gain is $1 + \mathcal{O}(T)$. In Figure 4.1, simulation is performed with choosing $c_0 = 1$, and $g = 0.25$, 0.5, and 0.75. We choose the sampling period h to be 0.0001s and have the random noise injected at the measurement of plant output.

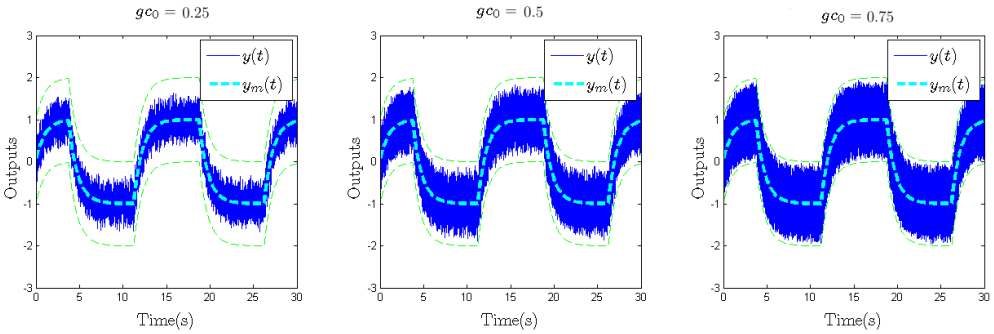

Figure 4.1: Fixed parameter simulation with $gc_0 \in (0, 1)$.

Since we choose $||n||_\infty = 1$, the maximum induced noise gain should be $1 + \mathcal{O}(T)$. Therefore, the outputs live in the envelope of $y_m(t) \pm (1 + \mathcal{O}(T))$. This can be observed from the above plot.

4.5.2 Example 2

From our previous results, we see that the noise is not amplified with smaller sampling periods. This is a very nice feature! In practice, running the system at a faster rate gives faster convergence. However, this is usually limited by the occurrence of the high frequency noise. Surprisingly, in our case, the system can run with the maximum possible sampling rate without worrying about the effect of the noise. In this simulation, we test this property by increasing the sample rate. Figure 4.2 plots the outputs with using sampling periods $h = 0.1$s, $h = 0.001$s, and $h = 0.00001$s. For these simulations, we choose $gc_0 = 0.75$ so that $\|T_{ny}\| = 1 + \mathcal{O}(T)$. As we can see, the outputs $y(t)$ are always inside the desired bound.

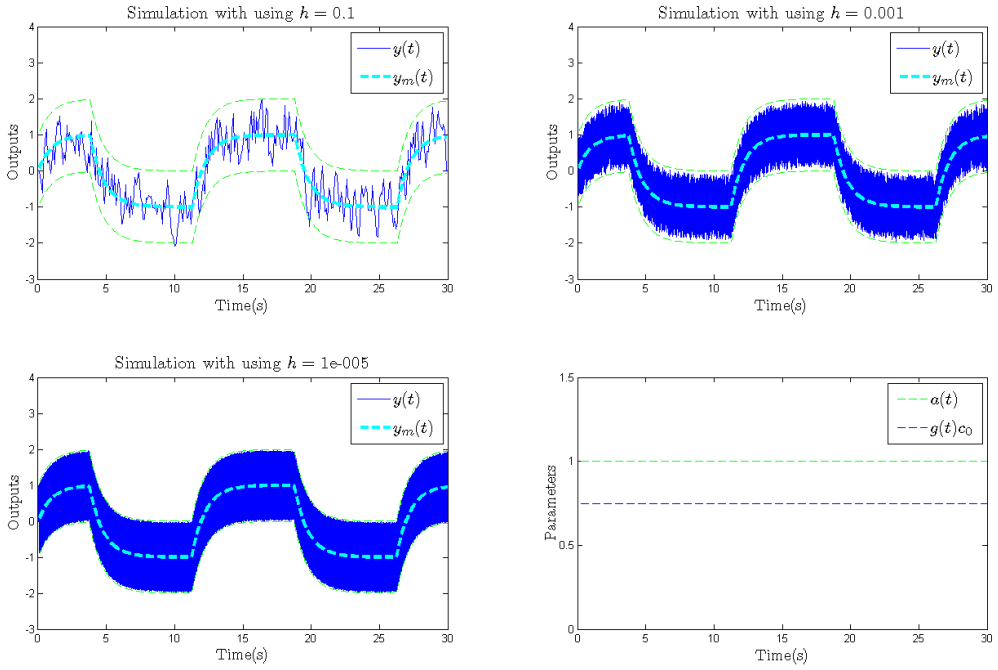

Figure 4.2: Fixed parameter simulation with using different sampling period.

Chapter 5

Time-varying Parameter Case

In the previous chapter, we derived an expression of the induced noise gain for the case where the plant is first order and linear time-invariant. The result shows that the induced noise gain is $1 + \mathcal{O}(T)$ when the controller parameters c_0 satisfies $c_0 \in (0, \frac{1}{\bar{g}})$, for then $gc_0 \in (0, 1)$ for all admissible g.

To extend the previous result, in this chapter we will look at the case with a first order time-varying plant. In particular, we assume the set of plant uncertainty to be

$$\bar{\mathcal{P}}_{ac}(n = 1, m = 1, \bar{\Gamma}, \bar{\mu}_1, \underline{g}, \gamma_0, \lambda_0),$$

and the plant is parametrized by $\bar{\theta}(t) = \begin{bmatrix} \beta_0(t) \\ g(t) \end{bmatrix}$. In the light of the previous result, we would like to find the induced noise gain when $g(t) \in [\underline{g}, \bar{g}]$ is time-varying and the controller parameters $c_0 \in (0, \frac{1}{\bar{g}})$. It turns out that the function $1 - g(t)c_0$ plays an important role in the analysis. If we set $\varepsilon := 1 - \underline{g}c_0$, then for all t,

$$\begin{aligned} 1 - g(t)c_0 &\in (1 - \bar{g}c_0, 1 - \underline{g}c_0) \\ &\in (0, 1 - \underline{g}c_0) \\ &= (0, \varepsilon). \end{aligned}$$

For simplicity, we also assumed that the plant parameters are continuous (Assumption 8). In other words, we will not consider the case where plant parameters can have infrequent jumps. Since the plant parameters are slowly time-varying compared to the sampling rate, we expect the induced noise gain to be bounded just like in the LTI case.

5.1 State Space representation with first order time-varying plant

To formulate the problem for the time-varying case, we first express the system in the state space representation. Since the plant is first order, the controller is linear time-invariant. This can be seen from (3.33). Hence, the model of the controller is exactly the same as (4.7). On the other hand, the plant model is linear time-varying. With $\begin{pmatrix} a(t) \\ g(t) \end{pmatrix} \in \bar{\Gamma}$ and $g(t) \in [\underline{g}, \bar{g}]$ for all $t \geq 0$, consider the first order time-varying plant[1]

$$\dot{y}(t) = a(t)y(t) + g(t)u(t). \tag{5.1}$$

For $t_1, t_2 \in \mathbb{R}^+$, denote the transition matrix of a time interval $[t_1, t_2]$ to be

$$\Phi(t_1, t_2) = e^{\int_{t_1}^{t_2} a(w)dw}.$$

Then, the discrete version of (5.1) is

$$y[(k+1)T] = \Phi\big((k+1)T, kT\big)y(kT) + \int_{kT}^{(k+1)T} \Phi((k+1)T, \tau)g(\tau)u(\tau)d\tau, \quad k \geq 0. \tag{5.2}$$

Due to the complexity of the transition matrix of a time-varying system, we will express (5.2) using the order notation. Applying **Lemma 3** from Appendix B, if we denote the discrete-time state space matrices to be

$$\begin{aligned} A_p(kT) &= 1 + a(kT)T + \mathcal{O}(T^2), \\ B_p(kT) &= Tg(kT) + \mathcal{O}(T^2), \\ C_p(kT) &= 1, \\ D_p(kT) &= 0, \end{aligned}$$

it follows that the discrete-time state space representation of the plant is

$$\begin{aligned} x_2[(k+1)T] &= A_p(kT)x_2(kT) + B_p(kT)u(kT), \quad x_2(0) = 0, \\ y(kT) &= C_p(kT)x_2(kT) + D_p(kT)u(kT). \end{aligned} \tag{5.3}$$

[1]Instead of using $\bar{\theta}(t) = \begin{bmatrix} \beta_0(t) \\ g(t) \end{bmatrix}$, we use $\bar{\theta}(t) = \begin{bmatrix} a(t) \\ g(t) \end{bmatrix}$ to embrace the natural notation of the first order linear time-varying plant $\dot{y}(t) = a(t)y(t) + g(t)u(t)$.

For the case where the plant is first order LTV, the controller is exactly the same as the one for a first order LTI plant. Hence, we will use the state-space representation as presented in (4.7) for the controller. For the closed-loop system, connect the controller and the plant in series. By combining (4.7) and (5.3), we have

$$\begin{aligned}\begin{pmatrix} x_1[(k+1)T] \\ x_2[(k+1)T] \end{pmatrix} &= \begin{bmatrix} A_c & 0 \\ B_p(kT)C_c & A_p(kT) \end{bmatrix} \begin{pmatrix} x_1(kT) \\ x_2(kT) \end{pmatrix} + \begin{bmatrix} B_c \\ B_p(kT)D_c \end{bmatrix} y_n(kT), \\ y(kT) &= \begin{bmatrix} D_p(kT)C_c & C_p(kT) \end{bmatrix} \begin{pmatrix} x_1(kT) \\ x_2(kT) \end{pmatrix} + \begin{bmatrix} D_p(kT)D_c \end{bmatrix} y_n(kT). \end{aligned} \tag{5.4}$$

Substituting the values of (A_c, B_c, C_c, D_c) and $(A_p(kT), B_p(kT), C_p(kT), D_p(kT))$, we have:

$$\begin{aligned}\begin{pmatrix} x_1[(k+1)T] \\ x_2[(k+1)T] \end{pmatrix} &= \begin{bmatrix} 1 & 0 \\ g(kT)c_0\bar{f}_2T + \mathcal{O}(T^2) & 1 + a(kT)T + \mathcal{O}(T^2) \end{bmatrix} \begin{pmatrix} x_1(kT) \\ x_2(kT) \end{pmatrix} + \\ &\quad \begin{bmatrix} 1 \\ -g(kT)c_0 + \mathcal{O}(T) \end{bmatrix} y_n(kT), \\ y(kT) &= \begin{bmatrix} 0 & 1 \end{bmatrix} \begin{pmatrix} x_1(kT) \\ x_2(kT) \end{pmatrix}. \end{aligned}$$

Since $x_2(kT) = y(kT)$ and $y_n(kT) = y(kT) + n(kT)$, the **state-space representation for the time-varying case** can be written as:

$$\begin{aligned}\begin{pmatrix} x_1[(k+1)T] \\ x_2[(k+1)T] \end{pmatrix} &= \underbrace{\begin{bmatrix} 1 & 1 \\ g(kT)c_0\bar{f}_2T + \mathcal{O}(T^2) & 1 - g(kT)c_0 + \mathcal{O}(T) \end{bmatrix}}_{=:A_{cl}(kT)} \underbrace{\begin{pmatrix} x_1(kT) \\ x_2(kT) \end{pmatrix}}_{=:x(kT)} + \\ &\quad \underbrace{\begin{bmatrix} 1 \\ -g(kT)c_0 + \mathcal{O}(T) \end{bmatrix}}_{=:B_{cl}(kT)} n(kT), \quad x(0) = 0, \\ y(kT) &= \underbrace{\begin{bmatrix} 0 & 1 \end{bmatrix}}_{=:C_{cl}(kT)} \begin{pmatrix} x_1(kT) \\ x_2(kT) \end{pmatrix}. \end{aligned}$$

5.1.1 The Transformed State $\bar{x}$

Unlike in the previous chapter, the closed-loop system is a linear time-varying system. Since the state matrices are time-varying, there is no easy way to diagonalize the system.

However, we can diagonalize the system at every time step. We use the same diagonalization method that is used in Chapter 4, and use

- $L(kT) = -\bar{f}_2 T + \mathcal{O}(T^2)$,
- $P(kT) = \frac{1}{g(kT)c_0} + \mathcal{O}(T)$;

we end up with a time-varying diagonalization matrix

$$\begin{aligned}\mathcal{T}(kT) &= \begin{bmatrix} 1 & -P(kT) \\ -L(kT) & 1 + P(kT)L(kT) \end{bmatrix} \\ &= \begin{bmatrix} 1 & -\frac{1}{g(kT)c_0} + \mathcal{O}(T) \\ \bar{f}_2 T + \mathcal{O}(T^2) & 1 - \frac{\bar{f}_2 T}{g(kT)c_0} + \mathcal{O}(T^2) \end{bmatrix}\end{aligned} \tag{5.5}$$

whose inverse is

$$\begin{aligned}\mathcal{T}^{-1}(kT) &= \begin{bmatrix} 1 + P(kT)L(kT) & P(kT) \\ L(kT) & 1 \end{bmatrix} \\ &= \begin{bmatrix} 1 - \frac{\bar{f}_2 T}{g(kT)c_0} + \mathcal{O}(T^2) & \frac{1}{g(kT)c_0} + \mathcal{O}(T) \\ -\bar{f}_2 T + \mathcal{O}(T^2) & 1 \end{bmatrix}.\end{aligned} \tag{5.6}$$

With $\Lambda(kT) := \mathcal{T}^{-1}(kT)A_{cl}(kT)\mathcal{T}(kT)$, the state equation of (5.5) can be written as

$$x[(k+1)T] = \mathcal{T}(kT)\Lambda(kT)\mathcal{T}^{-1}(kT)x(kT) + B_{cl}(kT)n(kT).$$

It follows that

$$\mathcal{T}^{-1}(kT)x[(k+1)T] = \Lambda(kT)\underbrace{\mathcal{T}^{-1}(kT)x(kT)}_{=:\bar{x}(kT)} + \mathcal{T}^{-1}(kT)B_{cl}(kT)n(kT).$$

Hence, the update equation for $\bar{x}$ is

$$\begin{aligned}\bar{x}[(k+1)T] &= \mathcal{T}^{-1}[(k+1)T]x[(k+1)T] \\ &= \mathcal{T}^{-1}[(k+1)T]\mathcal{T}(kT)\Lambda(kT)\bar{x}(kT) + \mathcal{T}^{-1}[(k+1)T]B_{cl}(kT)n(kT) \\ &= \big[\Lambda(kT) + \underbrace{(\mathcal{T}^{-1}[(k+1)T]\mathcal{T}(kT) - I)\Lambda(kT)}_{=:\Delta_1(kT)}\big]\bar{x}(kT) + \\ &\quad \big[\mathcal{T}^{-1}(kT)B_{cl}(kT) + \underbrace{(\mathcal{T}^{-1}[(k+1)T] - \mathcal{T}^{-1}(kT))B_{cl}(kT)}_{=:\Delta_2(kT)}\big]n(kT).\end{aligned}$$

It turns out that all of the matrices in this equation have a rich structure:

$$\begin{aligned}
\Lambda(kT) &= \mathcal{T}^{-1}(kT)A_{cl}(kT)\mathcal{T}(kT) \\
&= \begin{bmatrix} 1+\bar{f}_2 T+\mathcal{O}(T^2) & 0 \\ 0 & 1-g(kT)c_0+\mathcal{O}(T) \end{bmatrix}, \\
\Delta_1(kT) &= (\mathcal{T}^{-1}[(k+1)T]\mathcal{T}(kT)-I)\Lambda(kT) \\
&= \begin{bmatrix} \mathcal{O}(T^2) & \mathcal{O}(T) \\ \mathcal{O}(T^2) & \mathcal{O}(T^2) \end{bmatrix}, \\
\mathcal{T}^{-1}(kT)B_{cl}(kT) &= \begin{bmatrix} \mathcal{O}(T) \\ -g(kT)c_0+\mathcal{O}(T) \end{bmatrix}, \\
\Delta_2(kT) &= (\mathcal{T}^{-1}[(k+1)T]-\mathcal{T}^{-1}(kT))B_{cl}(kT) \\
&= \begin{bmatrix} \mathcal{O}(T) \\ \mathcal{O}(T^2) \end{bmatrix}.
\end{aligned} \tag{5.7}$$

For notational simplicity, denote

$$\bar{A}_{cl}(kT) := \Lambda(kT)+\Delta_1(kT),$$

and

$$\bar{B}_{cl}(kT) := \mathcal{T}^{-1}(kT)B_{cl}(kT)+\Delta_2(kT).$$

The update equation of the $\bar{x}$ system becomes

$$\bar{x}[(k+1)T] = \bar{A}_{cl}(kT)\bar{x}(kT)+\bar{B}_{cl}(kT)n(kT). \tag{5.8}$$

Furthermore, the output equation of the $\bar{x}$ system can be written as

$$y(kT) = \underbrace{C_{cl}(kT)\mathcal{T}(kT)}_{:=\bar{C}_{cl}(kT)}\bar{x}(kT), \tag{5.9}$$

with

$$\begin{aligned}
\bar{C}_{cl}(kT) &= C_{cl}(kT)\mathcal{T}(kT) \\
&= \begin{bmatrix} 0 & 1 \end{bmatrix}\begin{bmatrix} 1 & -\frac{1}{g(kT)c_0}+\mathcal{O}(T) \\ \bar{f}_2 T+\mathcal{O}(T^2) & 1-\frac{\bar{f}_2 T}{g(kT)c_0}+\mathcal{O}(T^2) \end{bmatrix} \\
&= \begin{bmatrix} \mathcal{O}(T) & 1+\mathcal{O}(T) \end{bmatrix}.
\end{aligned}$$

Combining all of the above, the $\bar{x}$ **system** can be written as:

$$\begin{aligned}
\bar{x}[(k+1)T] &= \bar{A}_{cl}(kT)\bar{x}(kT)+\bar{B}_{cl}(kT)n(kT), \quad \bar{x}(0)=0, \\
y(kT) &= \bar{C}_{cl}(kT)\bar{x}(kT),
\end{aligned} \tag{5.10}$$

with $\bar{A}_{cl}(kT)$ and $\bar{B}_{cl}(kT)$ shown in (5.8) and $\bar{C}_{cl}(kT)$ shown in (5.9).

5.2 Analyzing the LTV system

In Chapter 4, where the LTI case was examined, we diagonalized the system to compute the induced noise gain. Unfortunately, for the time-varying case, we are unable to do so because state space matrices are time-varying so the diagonalization matrix is not constant. In the previous section, we derived the difference equation for the transformed state $\bar{x}$, and $\bar{A}_{cl}(kT)$ is not purely diagonal. In this section, we first find a weak bound in the state $\bar{x}$, which we then leverage to obtain tighter bounds. Eventually, we derive the desired bound.

5.2.1 Stability

Since $\bar{A}_{cl}(kT)$ is not diagonal, we cannot separate the 'fast' and 'slow' mode of the closed-loop system. Note that the two eigenvalues of $\bar{A}_{cl}(kT)$ are roughly at $1 + \bar{f}_2 T$ and $1 - g(kT)c_0$, which, for small T, are inside the unit disk. However, the stability/instability of a linear time-varying system cannot be determined from the eigenvalues of $\bar{A}_{cl}(kT)$ as demonstrated [4].

In this section, we will first find a bound on $\|\bar{A}_{cl}(kT)\|$. Since $\bar{A}_{cl}(kT)$ is 'almost' in the diagonal form, we expect that the bound of $\|\bar{A}_{cl}(kT)\|$ is closely related to the slow mode $(1 + \bar{f}_2 T)$ of the system.

Claim 2. *With $\tilde{f}_2$ a negative constant satisfying $\tilde{f}_2 \in (\bar{f}_2, 0)$, we have*

$$||\bar{A}_{cl}(kT)|| < e^{\tilde{f}_2 T}, \quad k \in \mathbb{Z}^+. \tag{5.11}$$

Proof. Consider

$$\bar{\mathcal{A}}(kT) := \bar{A}_{cl}(kT)\big(e^{-\tilde{f}_2 T} I\big)$$

Recall that

$$\|\bar{\mathcal{A}}(kT)\| < 1 \quad \Longleftrightarrow \quad I - \bar{\mathcal{A}}^T(kT)\bar{\mathcal{A}}(kT) > 0.$$

But

$$\begin{aligned}
\bar{\mathcal{A}}(kT) &= \bar{A}_{cl}(kT)\big(e^{-\tilde{f}_2 T} I\big) \\
&= \big(\Lambda(kT) + \Delta_1(kT)\big)\big(e^{-\tilde{f}_2 T} I\big) \\
&= \begin{bmatrix} 1 + \bar{f}_2 T + \mathcal{O}(T^2) & \mathcal{O}(T) \\ \mathcal{O}(T^2) & 1 - g(kT)c_0 + \mathcal{O}(T) \end{bmatrix} \begin{bmatrix} 1 - \tilde{f}_2 T + \mathcal{O}(T^2) & 0 \\ 0 & 1 - \tilde{f}_2 T + \mathcal{O}(T^2) \end{bmatrix} \\
&= \begin{bmatrix} 1 + (\bar{f}_2 - \tilde{f}_2)T + \mathcal{O}(T^2) & \mathcal{O}(T) \\ \mathcal{O}(T^2) & 1 - g(kT)c_0 + \mathcal{O}(T) \end{bmatrix}.
\end{aligned}$$

So it follows that

$$\begin{aligned}
I - \bar{\mathcal{A}}(kT)^T\bar{\mathcal{A}}(kT) &= I - \left[\begin{array}{cc} 1+(\bar{f}_2-\tilde{f}_2)T+\mathcal{O}(T^2) & \mathcal{O}(T^2) \\ \mathcal{O}(T) & 1-g(kT)c_0+\mathcal{O}(T) \end{array}\right]\cdot \\
&\quad \left[\begin{array}{cc} 1+(\bar{f}_2-\tilde{f}_2)T+\mathcal{O}(T^2) & \mathcal{O}(T) \\ \mathcal{O}(T^2) & 1-g(kT)c_0+\mathcal{O}(T) \end{array}\right] \\
&= I - \left[\begin{array}{cc} (1+(\bar{f}_2-\tilde{f}_2)T)^2+\mathcal{O}(T^2) & \mathcal{O}(T) \\ \mathcal{O}(T) & (1-g(kT)c_0)^2+\mathcal{O}(T) \end{array}\right] \\
&= \left[\begin{array}{cc} 1-\left[1+(\bar{f}_2-\tilde{f}_2)T\right]^2+\mathcal{O}(T^2) & \mathcal{O}(T) \\ \mathcal{O}(T) & 1-(1-g(kT)c_0)^2+\mathcal{O}(T) \end{array}\right] \\
&= \left[\begin{array}{cc} -2\left(\bar{f}_2-\tilde{f}_2\right)T+\mathcal{O}(T^2) & \mathcal{O}(T) \\ \mathcal{O}(T) & 2g(kT)c_0+(g(kT)c_0)^2+\mathcal{O}(T^2) \end{array}\right].
\end{aligned}$$

Following the definition of $\tilde{f}_2$, we have $(\bar{f}_2-\tilde{f}_2)<0$. Since we choose c_0 so that $g(kT)c_0 \in [\underline{g}c_0, \bar{g}c_0] \subset (0,1)$, then there exist positive constants γ_3 and a time-varying function $\gamma_4(kT)$ such that:

- $\gamma_3 := -2(\bar{f}_2-\tilde{f}_2) > 0$,
- $\gamma_4(kT) := 2g(kT)c_0 + c_0^2 g(kT)^2 \geq 2\underline{g}c_0 + c_0^2\underline{g}^2 > 0$,

and

$$I - \bar{\mathcal{A}}(kT)^T\bar{\mathcal{A}}(kT) = \left[\begin{array}{cc} \gamma_3 T+\mathcal{O}(T^2) & \mathcal{O}(T) \\ \mathcal{O}(T) & \gamma_4(kT)+\mathcal{O}(T) \end{array}\right].$$

Hence, for small T, the leading principal minors are:

- $\gamma_3 T + \mathcal{O}(T^2) > 0$,
- $\big(\gamma_3 T+\mathcal{O}(T^2)\big)\big(\gamma_4(kT)+\mathcal{O}(T)\big) - \mathcal{O}(T^2) \geq (\gamma_3 T+\mathcal{O}(T^2))(2\underline{g}c_0+\underline{g}^2c_0^2+\mathcal{O}(T)) - \mathcal{O}(T^2)$
  $= (2\underline{g}c_0+\underline{g}^2c_0^2)\gamma_3 T + \mathcal{O}(T^2)$
  $> 0.$

Since all the leading principal minors are positive, we conclude that for small T, $I - \bar{\mathcal{A}}(kT)^T\bar{\mathcal{A}}(kT)$ is positive definite, or equivalently,

$$||\bar{\mathcal{A}}(kT)|| < 1,\ k \in \mathbb{Z}^+. \tag{5.12}$$

It follows immediately that for small T,

$$\|\bar{A}_{cl}(kT)\| < e^{\tilde{f}_2 T},\ k \in \mathbb{Z}^+,$$

as required. □

The above result gives us a bound on $\|\bar{A}_{cl}(kT)\|$. This gives us information about 'how fast' the $\bar{x}$ system converges. Now, the solution of (5.10) can be written as

$$\bar{x}[(k+1)T] = \left(\prod_{i=1}^{k} \bar{A}_{cl}(iT)\right) \bar{B}_{cl}(0)n(0) + \left(\prod_{i=2}^{k} \bar{A}_{cl}(iT)\right) \bar{B}_{cl}(T)n(T) + \cdots + \bar{A}_{cl}(kT)\bar{B}_{cl}[(k-1)T]n[(k-1)T] + \bar{B}_{cl}(kT)n(kT).$$

If we set $\gamma_5 = \bar{g}c_0 + 1$, it follows that for small T, we have

$$\|\bar{B}_{cl}(kT)\| \leq \gamma_5, \quad k \geq 0.$$

If we take the vector norm on both sides of the above equation and use the fact that $\|\bar{A}_{cl}\|_\infty < e^{\tilde{f}_2 T} < 1$, $k \geq 0$, and $\|n(kT)\| \leq \|n\|_\infty$, we end up with

$$\begin{aligned}
\|\bar{x}[(k+1)T]\| \leq & \left(e^{\tilde{f}_2 T}\right)^k \|\bar{B}_{cl}(0)\||n(0)| + \left(e^{\tilde{f}_2 T}\right)^{k-1} \|\bar{B}_{cl}(T)\||n(T)| + \cdots + \\
& \left(e^{\tilde{f}_2 T}\right)^1 \|\bar{B}_{cl}[(k-1)T]\||n[(k-1)T]| + \left(e^{\tilde{f}_2 T}\right)^0 \|\bar{B}_{cl}(kT)\||n(kT)| \\
\leq & \gamma_5 \sum_{i=0}^{k} \left(e^{\tilde{f}_2 T}\right)^i ||n||_\infty \\
\leq & \gamma_5 \sum_{i=0}^{\infty} \left(e^{\tilde{f}_2 T}\right)^i ||n||_\infty \\
\leq & \gamma_5 \frac{1}{1 - e^{\tilde{f}_2 T}} ||n||_\infty \\
\leq & \gamma_5 \frac{1}{-\tilde{f}_2 T + \mathcal{O}(T^2)} ||n||_\infty, \quad k \geq 0.
\end{aligned}$$

Hence, for small T we see that

$$||\bar{x}(kT)|| \leq \frac{2\gamma_5}{|\tilde{f}_2|T} ||n||_\infty, \quad k \geq 0. \tag{5.13}$$

In the next section, we are going to use this weak bound to obtain better bounds.

5.2.2 Tighter bounds

If we take a look at the state equation of the $\bar{x}$ system in detail, we have

$$\begin{pmatrix} \bar{x}_1(k+1)T \\ \bar{x}_2(k+1)T \end{pmatrix} = \begin{bmatrix} 1+\bar{f}_2T+\mathcal{O}(T^2) & \mathcal{O}(T) \\ \mathcal{O}(T^2) & 1-g(kT)c_0+\mathcal{O}(T) \end{bmatrix} \begin{pmatrix} \bar{x}_1(kT) \\ \bar{x}_2(kT) \end{pmatrix} + \begin{pmatrix} \mathcal{O}(T) \\ -g(kT)c_0+\mathcal{O}(T) \end{pmatrix} n(kT),$$

where the dynamics governing $\bar{x}_1$ is closely related to $1+\bar{f}T$ and the dynamics governing $\bar{x}_2$ is closely related to $1-g(kT)c_0$. In the following, we are going to look at the updated equation of $\bar{x}_1$ and $\bar{x}_2$ separately. First, by examining the $\bar{x}_2$ equation, we have

$$\bar{x}_2[(k+1)T] = \mathcal{O}(T^2)\bar{x}_1(kT) + \big(1-g(kT)c_0+\mathcal{O}(T)\big)\bar{x}_2(kT) + \big(-g(kT)c_0+\mathcal{O}(T)\big)n(kT).$$

Using (5.13) and the fact that $|g(kT)c_0| \leq 1$ for all $k \geq 0$, we have

$$\begin{aligned} \bar{x}_2[(k+1)T] &\leq \mathcal{O}(T)||n||_\infty + \big(1-g(kT)c_0+\mathcal{O}(T)\big)\bar{x}_2(kT) + \mathcal{O}(1)||n||_\infty \\ &= \big(1-g(kT)c_0+\mathcal{O}(T)\big)\bar{x}_2(kT) + \mathcal{O}(1)||n||_\infty. \end{aligned}$$

Since $\varepsilon = 1-\underline{g}c_0$ and we choose c_0 so that $g(kT)c_0 \in [1-\varepsilon, \bar{g}c_0] \subset (0,1)$ for all $k \geq 0$, it follows that there exists a constant γ_7 such that for small T

$$|\bar{x}_2[(k+1)T]| \leq \left(1-\frac{1-\varepsilon}{2}\right)^k |\bar{x}_2(kT)| + \gamma_7||n||_\infty, \tag{5.14}$$

which means that

$$|\bar{x}_2(kT)| \leq \left(1-\frac{1-\varepsilon}{2}\right)^k |\bar{x}_2(0)| + \frac{2\gamma_7}{1-\varepsilon}||n||_\infty. \tag{5.15}$$

With zero initial condition, we have

$$|\bar{x}_2(kT)| \leq \frac{2\gamma_7}{1-\varepsilon}||n||_\infty, \quad k \geq 0. \tag{5.16}$$

Hence,

$$\sup_{k\geq 0} ||\bar{x}_2(kT)|| = \mathcal{O}(1)||n||_\infty, \tag{5.17}$$

which a tighter bound for $\bar{x}_2$.

Now we will obtain even tighter bounds on both $\bar{x}_1$ and $\bar{x}_2$. The state equation for $\bar{x}_1$ is

$$\bar{x}_1[(k+1)T] \;=\; \big(1+\bar{f}_2T+\mathcal{O}(T^2)\big)\bar{x}_1(kT)+\mathcal{O}(T)\bar{x}_2(kT)+\mathcal{O}(T)n(kT).$$

Since $|\bar{x}_2(kT)|=\mathcal{O}(1)||n||_\infty$ and $|n(kT)|\le||n||_\infty$ for all $k\ge0$, then there exists a positive constant γ_8 such that for small T

$$|\bar{x}_1[(k+1)T]| \;\le\; \left(1+\tfrac{\bar{f}_2T}{2}\right)|\bar{x}_1(kT)|+\gamma_8T||n||_\infty,\quad k\ge0. \tag{5.18}$$

Hence,

$$\begin{aligned}|\bar{x}_1(kT)| &\le \left(1+\tfrac{\bar{f}_2T}{2}\right)^k|\bar{x}_1(0)|+\textstyle\sum_{i=0}^{k-1}\left(1+\tfrac{\bar{f}_2T}{2}\right)^i\gamma_8T||n||_\infty\\ &\le \left(1+\tfrac{\bar{f}_2T}{2}\right)^k|\bar{x}_1(0)|+\textstyle\sum_{i=0}^{\infty}\left(1+\tfrac{\bar{f}_2T}{2}\right)^i\gamma_8T||n||_\infty.\end{aligned}$$

Following the definition of $\bar{f}_2$, we have $0<1+\frac{\bar{f}_2T}{2}<1$. Then, with zero initial conditions, we have that for small T

$$|\bar{x}_1(kT)|\le\frac{2\gamma_8}{|\bar{f}_2|}||n||_\infty,\quad k\ge0. \tag{5.19}$$

Hence, for small T

$$\sup_{k\ge0}\|\bar{x}_1(kT)\|=\mathcal{O}(1)\|n\|_\infty. \tag{5.20}$$

Next, we will prove the tighter bounds on $\bar{x}_2$ using induction. As alone, by examining the $\bar{x}_2$ equation we have

$$\begin{aligned}\bar{x}_2[(k+1)T] &= [1-g(kT)+\mathcal{O}(T)]\,\bar{x}_2(kT)+\mathcal{O}(T^2)\bar{x}_1(kT)+[-g(kT)c_0+\mathcal{O}(T)]\\ &= [1-g(kT)c_0]\,\bar{x}_2(kT)-g(kT)c_0n(kT)+\\ &\quad\underbrace{\mathcal{O}(T^2)\bar{x}_1(kT)+\mathcal{O}(T)\bar{x}_2(kT)+\mathcal{O}(T)n(kT)}_{=:\Delta_3(kT)}\end{aligned} \tag{5.21}$$

Using the bound on $\|\bar{x}_1\|_\infty$ given in (5.20) and the bound on $\|\bar{x}_2\|_\infty$ given by (5.17), it follows that there exists a constant γ_9 such that for small T,

$$\|\Delta_3(kT)\|\le\gamma_9T\|n\|_\infty,\quad k\ge0.$$

Suppose $\bar{x}_2(0)=0$; we claim that for small T,

$$\|\bar{x}_2(kT)\|\le\left(1+\frac{\gamma_9}{1-\varepsilon}T\right)\|n\|_\infty,\quad k\ge0. \tag{5.22}$$

To prove this, suppose that it is true for $k = 0, 1, \cdots j$; then

$$\begin{aligned}
|\bar{x}_2[(j+1)T]| &\leq |1 - g(jT)c_0||\bar{x}_2(jT)| + |g(jT)c_0|\|n\|_\infty + \gamma_9 T\|n\|_\infty \\
&\leq |1 - g(jT)c_0|(1 + \tfrac{\gamma_9}{1-\varepsilon}T)\|n\|_\infty + |g(jT)c_0|\|n\|_\infty + \gamma_9 T\|n\|_\infty \\
&\leq \underbrace{(|1 - g(jT)c_0| + |g(jT)c_0|)}_{=1}\|n\|_\infty + \varepsilon\tfrac{\gamma_9}{1-\varepsilon}T\|n\|_\infty + \gamma_9 T\|n\|_\infty \\
&\leq \left[1 + \gamma_9\left(1 + \tfrac{\varepsilon}{1-\varepsilon}\right)T\right]\|n\|_\infty \\
&= \left(1 + \tfrac{\gamma_9}{1-\varepsilon}T\right)\|n\|_\infty,
\end{aligned} \tag{5.23}$$

as desired. We conclude that

$$\sup_{k\geq 0}\|\bar{x}_2(kT)\| = (1 + \mathcal{O}(T))\,\|n\|_\infty. \tag{5.24}$$

5.2.3 Maximum Noise Gain (Time-varying Case)

Using the results from (5.20) and (5.24) and substituting into (5.9), we have

$$\begin{aligned}
|y(kT)| &= \left|C_{cl}(kT)\mathcal{T}(kT)\bar{x}(kT)\right| \\
&\leq \mathcal{O}(T)\sup_{k\geq 0}\|\bar{x}_1(kT)\| + (1 + \mathcal{O}(T))\sup_{k\geq 0}\|\bar{x}_2(kT)\| \\
&= \left(1 + \mathcal{O}(T)\right)||n||_\infty, \quad k \in \mathbb{Z}^+.
\end{aligned} \tag{5.25}$$

Hence, the output is well behaved at the sample points.

Now, we will show that the output is also well behaved in between the sample points. Since $x(kT) = \mathcal{T}(kT)\bar{x}(kT)$, if we use the bound found for $\bar{x}$, we have

$$\begin{aligned}
x(kT) &= \mathcal{T}(kT)\bar{x}(kT) \\
&= \begin{bmatrix} 1 & -\frac{1}{g(kT)c_0} + \mathcal{O}(T) \\ \bar{f}_2 T & 1 - \frac{\bar{f}_2 T}{g(kT)c_0 + \mathcal{O}(T^2)} \end{bmatrix} \begin{pmatrix} \mathcal{O}(1) \\ 1 + \mathcal{O}(T) \end{pmatrix} \|n\|_\infty \\
&= \begin{pmatrix} \mathcal{O}(1) \\ 1 + \mathcal{O}(T) \end{pmatrix} \|n\|_\infty, \quad k \geq 0,
\end{aligned}$$

so, in particular,

$$x_1(kT) = \mathcal{O}(1)\|n\|_\infty, \quad k \geq 0.$$

Substituting the above into the output equation of (4.7), we have

$$u(kT) = \mathcal{O}(1)\|n\|_\infty + \left(\frac{1}{T}\right)(-c_0)(y(kT) + n(kT)), \quad k \geq 0.$$

Using (5.25), it follows that

$$\begin{aligned}\sup_{k\geq 0}|u(kT)| &= \mathcal{O}(T)\|n\|_\infty + \mathcal{O}\left(\tfrac{1}{T}\right)\left[(1+\mathcal{O}(T))\|n\|_\infty + \|n\|_\infty\right] \\ &= \mathcal{O}\left(\tfrac{1}{T}\right)\|n\|_\infty.\end{aligned}$$

Note from the above that the bound on the control input is inversely proportional to the sampling period. Hence, sampling faster could cause a large control signal, which is the case in practice. Now, let's look at the output equation of (5.1). Using the previously defined transition matrix, the solution of (5.1) for $t \in [kT, (k+1)T)$ is

$$y(t) = \Phi\big(t, kT\big)y(kT) + \int_{kT}^{t} \Phi(t,\tau)g(\tau)u(\tau)d\tau, \quad k \geq 0. \tag{5.26}$$

Since we are using the sample-data controller, then for $t \in [kT, (k+1)T)$, $u(t) = u(kT)$. Since $\begin{bmatrix} a \\ g \end{bmatrix}$ lie in a compact set $\bar{\Gamma}$, there exist constants $\bar{a}$ and $\bar{g}$ such that

$$\|a\|_\infty \leq \bar{a} \quad \text{and} \quad \|g\|_\infty \leq \bar{g}.$$

It is easy to see that

$$\Phi(t,\tau) = 1 + \mathcal{O}(T), \quad kT \leq \tau \leq t \leq (k+1)T, \quad k \in \mathbb{Z}^+.$$

Using Lemma 2 from Appendix B, we have

$$g(\tau) = g(kT) + \mathcal{O}(T).$$

Using the above results in (5.26), we end up with

$$\begin{aligned} y(t) &= (1+\mathcal{O}(T))y(kT) + (t-kT)(g(kT)+\mathcal{O}(T))u(kT) \\ &= [y(kT) + (t-kT)g(kT)u(kT)] + \\ &\quad \big[\mathcal{O}(T)y(kT) + \mathcal{O}(T^2)u(kT)\big], \quad t \in [kT, (k+1)T]. \end{aligned} \tag{5.27}$$

Hence,

$$|y(t) - [y(kT) + (t-kT)g(kT)u(kT)]| = \mathcal{O}(T)\|n\|_\infty, \quad t \in [kT, (k+1)T], k \geq 0.$$

This means, in particular, that

$$\Big|y[(k+1)T] - \big[y(kT) + Tg(kT)u(kT)\big]\Big| = \mathcal{O}(T)\|n\|_\infty, \quad k \geq 0,$$

so

$$\Big|\big[y[(k+1)T]-y(kT)\big]+Tg(kT)u(kT)\Big|=\mathcal{O}(T)\|n\|_\infty,\quad k\geq 0.$$

Hence,

$$\begin{aligned}&\Big|y(t)-y(kT)-\tfrac{t-kT}{T}\left(y[(k+1)T]-y(kT)\right)\Big|\\ =\;&\Big|y(t)-y(kT)-(t-kT)g(kT)u(kT)\Big|+\mathcal{O}(T)\|n\|_\infty\\ =\;&\mathcal{O}(T)\|n\|_\infty,\quad t\in[kT,(k+1)T].\end{aligned}$$

However,

$$\left|y(kT)+\frac{t-kT}{T}(y[(k+1)T]-y(kT))\right|\leq\max\{|y(kT)|,|y[(k+1)T]|\},t\in[kT,(k+1)T],k\in\mathbb{Z}^+,$$

so

$$|y(t)|\leq\sup_{k\geq 0}|y(kT)|+\mathcal{O}(T)\|n\|_\infty,t\in[kT,(k+1)T],k\in\mathbb{Z}^+.$$

Using (5.25), we conclude that

$$\|y\|_\infty=(1+\mathcal{O}(T))\|n\|_\infty. \tag{5.28}$$

Since $n\in PC_\infty$ is arbitrary, it follows that

$$\|T_{ny}\|=1+\mathcal{O}(T), \tag{5.29}$$

which leads to our second main result.

Proposition 2. *For a first order time-invariant plant of the form (5.1) with known sign of the high frequency gain, using controller (3.21)-(3.25), the maximum induced noise gain is bounded. In particular, if the selection of c_0 satisfies $c_0\in(0,\frac{1}{\bar{g}})$, then for every $\delta>0$, there exists a $\bar{T}>0$ such that for every $T\in(0,\bar{T})$ and $\bar{\theta}\in\bar{\mathcal{P}}_{ac}(n=1,m=1,\bar{\Gamma},\bar{\mu}_1,\underline{g},\gamma_0,\lambda_0)$ for all $t\geq 0$, we have*

$$\|T_{ny}(\bar{\theta},T)\|\leq 1+\delta. \tag{5.30}$$

Until now, we showed that the maximum induced noise gain can be controlled to be $1+\mathcal{O}(T)$ if the plant is first order and linear time-varying. This leads to a natural question - can we still control the induced noise gain if the plant order is two or higher? In the next chapter, we are going to look at a more general case; we are going to look at the case where the plant is time-varying and with relative degree one.

Chapter 6

General Case

In the previous chapter, we examined the induced noise gain for the case where the plant is first order and time-varying. In this chapter, we will extend the result to the relative degree one case. In particular, we assume the set of plant uncertainties to be

$$\bar{\mathcal{P}}_{ac}(n, m = 1, \bar{\Gamma}, \bar{\mu}_1, \underline{g}, \gamma_0, \lambda_0),$$

and the plant is parameterized by

$$\bar{\theta}(t) := \begin{bmatrix} \alpha_0(t) & \cdots & \alpha_{n-2}(t) & \beta_0(t) & b_0(t) & \cdots & b_{n-2}(t) & g(t) \end{bmatrix}^T.$$

As we did in Chapter 5, we will look at the induced noise gain when $g(t) \in [\underline{g}, \bar{g}]$ is time-varying and the selection of c_0 satisfies $g(t)c_0 \in (0, 1)$ for all $t \geq 0$, namely $c_0 \in (0, \frac{1}{\bar{g}})$. Also, we still set $\varepsilon = 1 - \underline{g}c_0$ so that $1 - g(t)c_0 \leq \varepsilon < 1$ for all $t \geq 0$. We expect to prove a similar result as we did in chapter 5. The intuition for why this works is that for the relative degree one case, the plant is the composition of a first order linear time-varying plant and the zero dynamics. The ideal controller, which inspired the design of the adaptive controller, is designed in such a way that the zero dynamics are decoupled from the rest of the system. In our case, since the controller is only an approximation of the ideal controller, the zero dynamics is not completely decoupled from the rest of the system; the zero dynamics is weakly coupled to a first order linear time-varying system. Since we are assuming that the zero dynamics is uniformly exponential stable (Assumption 5), the 'weak' connection between the first order linear time-varying plant and the zero dynamics should not affect the plant output much.

6.1 State-Space Representation

As in the previous chapters, we write the plant and the controller in the state-space representation and then construct the closed-loop system. First, let's look at the relative degree one plant.

6.1.1 Relative Degree One Plant

For the relative degree one case, $m = 1$. Hence, the input output model of (3.1) becomes

$$\begin{array}{rcl} \sum_{i=0}^{n} a_i(t) D^i \eta & = & g(t) u \\ y & = & \sum_{i=0}^{n-1} b_i(t) D^i \eta. \end{array} \tag{6.1}$$

Using (3.14), the state-space representation of the relative degree one plant can be represented as[1]:

$$\begin{pmatrix} \dot{w} \\ \dot{v} \end{pmatrix} = \underbrace{\begin{bmatrix} \overbrace{\begin{bmatrix} & 1 & & \\ & & \ddots & \\ & & & 1 \\ -b_0(t) & -b_1(t) & \cdots & -b_{n-m-1}(t) \end{bmatrix}}^{A_1(t)} & \overbrace{\begin{bmatrix} 0 \\ \vdots \\ 0 \\ 1 \end{bmatrix}}^{b_1} \\ \underbrace{\begin{bmatrix} \alpha_0(t) & \alpha_1(t) & \cdots & \alpha_{n-m-1}(t) \end{bmatrix}}_{c_1(t)} & \underbrace{[-\beta_0(t)]}_{A_2(t)} \end{bmatrix}}_{=:A_{pc}(t)} \begin{pmatrix} w \\ v \end{pmatrix} + \underbrace{\begin{bmatrix} \begin{bmatrix} 0 \\ 0 \\ \vdots \\ 0 \end{bmatrix} \\ [g(t)] \end{bmatrix}}_{=:B_{pc}(t)} u,$$

$$y = \underbrace{\begin{bmatrix} \begin{bmatrix} 0 & 0 & \cdots & 0 \end{bmatrix} & [1] \end{bmatrix}}_{=:C_{pc}(t)} \begin{pmatrix} w \\ v \end{pmatrix}, \tag{6.2}$$

where the state $w = \begin{bmatrix} \eta \\ D\eta \\ \vdots \\ D^{n-2}\eta \end{bmatrix}$ is associated with the zero dynamics. Since $m = 1$, we have $y = v$. Note that all the time-varying elements of $A_{pc}(t)$ and $B_{pc}(t)$ (or $\bar{\theta}(t)$) are inside the compact set $\bar{\Gamma}$. In addition, we assume that $g(t) \in [\underline{g}, \bar{g}]$ for all $t \geq 0$.

[1]The notation here is consistent with (3.14). For the relative degree one case, we also have $b_2 = c_2 = 1$.

To discretize the plant, we use the result of **Lemma 3** from Appendix B. Applying Lemma 3 to (6.2) yields:

$$\begin{array}{rcl} \left(\begin{array}{c} w[(k+1)T] \\ v[(k+1)T] \end{array} \right) & = & (I + A_{pc}(kT)T + \mathcal{O}(T^2)) \left(\begin{array}{c} w(kT) \\ v(kT) \end{array} \right) + (B_{pc}(kT)T + \mathcal{O}(T^2))\, u(kT), \\ y(kT) & = & C_{pc} x_2(kT). \end{array} \tag{6.3}$$

If we break down the equation, we have:

$$\begin{array}{rcl} w[(k+1)T] & = & (I + A_1(kT)T + \mathcal{O}(T^2))\, w(kT) + (Tb_1 + \mathcal{O}(T^2))\, v(kT) + \mathcal{O}(T^2) u(kT), \\ v[(k+1)T] & = & (1 + A_2(kT)T + \mathcal{O}(T^2))\, v(kT) + (Tc_1(kT) + \mathcal{O}(T^2))\, w(kT) + \\ & & (Tg(kT) + \mathcal{O}(T^2))\, u(kT). \end{array}$$

Denote the state of the discretized plant by $x_2(kT) := \left(\begin{array}{c} v(kT) \\ w(kT) \end{array} \right)$ (Note that the order of v and w is switched). With

$$\begin{array}{rcl} A_p(kT) & := & \left[\begin{array}{cc} 1 + A_2(kT)T + \mathcal{O}(T^2) & Tc_1(kT) + \mathcal{O}(T^2) \\ Tb_1 + \mathcal{O}(T^2) & I + A_1(kT)T + \mathcal{O}(T^2) \end{array} \right], \\ B_p(kT) & := & \left[\begin{array}{c} Tg(kT) + \mathcal{O}(T^2) \\ \mathcal{O}(T^2) \end{array} \right], \quad \text{and} \\ C_p(kT) & := & \left[\begin{array}{cccc} 1 & 0 & \cdots & 0 \end{array} \right], \end{array}$$

and zero initial conditions, the discrete time state-space representation of the plant is:

$$\begin{array}{rcl} x_2[(k+1)T] & = & A_p(kT) x_2(kT) + B_p(kT) u(kT),\ x_2(0) = 0, \\ y(kT) & = & C_p(kT) x_2(kT). \end{array} \tag{6.4}$$

Combining the controller in (4.7) and the plant in (6.4), the closed-loop system state-space representation is:

$$\begin{array}{rcl} \left(\begin{array}{c} x_1[(k+1)T] \\ x_2[(k+1)T] \end{array} \right) & = & \left[\begin{array}{cc} A_c & 0 \\ B_p(kT)C_c & A_p(kT) \end{array} \right] \left(\begin{array}{c} x_1(kT) \\ x_2(kT) \end{array} \right) + \left[\begin{array}{c} B_c \\ B_p(kT)D_c \end{array} \right] y_n(kT), \\ y(kT) & = & \left[\begin{array}{cc} 0 & C_p(kT) \end{array} \right] \left(\begin{array}{c} x_1(kT) \\ x_2(kT). \end{array} \right) \end{array}$$

Since $y_n(kT) = y(kT) + n(kT)$ and $y(kT) = C_p(kT)x_2(kT)$, we have

$$\begin{aligned}
\begin{pmatrix} x_1[(k+1)T] \\ x_2[(k+1)T] \end{pmatrix} &= \underbrace{\begin{bmatrix} A_c & B_cC_p(kT) \\ B_p(kT)C_c & A_p(kT) + B_p(kT)D_cC_p(kT) \end{bmatrix}}_{=:A_{cl}(kT)} \begin{pmatrix} x_1(kT) \\ x_2(kT) \end{pmatrix} + \\
&\quad \underbrace{\begin{bmatrix} B_c \\ B_p(kT)D_c \end{bmatrix}}_{=:B_{cl}(kT)} n(kT). \\
y(kT) &= \underbrace{\begin{bmatrix} 0 & C_p(kT) \end{bmatrix}}_{=:C_{cl}(kT)} \begin{pmatrix} x_1(kT) \\ x_2(kT) \end{pmatrix}.
\end{aligned}$$

Note that for the above state space representation, noise is the only system input. If we substitute the value of (A_c, B_c, C_c, D_c) and $(A_p(kT), B_p(kT), C_p(kT))$, then the state matrices are

$$\begin{aligned}
A_{cl}(kT) &= \begin{bmatrix} 1 & 1 & 0 \\ Tc_0\bar{f}_2 g(kT) + \mathcal{O}(T^2) & 1 - c_0 g(kT) + \mathcal{O}(T^2) & c_1(kT)T + \mathcal{O}(T^2) \\ \mathcal{O}(T^2) & \mathcal{O}(T) & I + A_1(kT)T + \mathcal{O}(T^2) \end{bmatrix}, \\
B_{cl}(kT) &= \begin{bmatrix} 1 \\ -c_0 g(kT) + \mathcal{O}(T) \\ \mathcal{O}(T) \end{bmatrix}, \\
C_{cl}(kT) &= \begin{bmatrix} 0 & 1 & 0 & \cdots & 0 \end{bmatrix}.
\end{aligned}$$

Hence, we end up with the **state-space representation of the closed-loop system**:

$$\begin{aligned}
x[(k+1)T] &= A_{cl}(kT)x(kT) + B_{cl}(kT)n(kT), \quad x(0) = 0, \\
y(kT) &= C_{cl}(kT)x(kT),
\end{aligned} \tag{6.5}$$

where the state $x(kT) = \begin{pmatrix} x_1(kT) \\ x_2(kT) \end{pmatrix} = \begin{pmatrix} x_1(kT) \\ v(kT) \\ w(kT) \end{pmatrix}$.

6.1.2 The Transformed State $\bar{x}$

In Chapter 5 where the plant is first order and time-varying, we did a similarity transformation to the closed-loop system so that the 'A' matrix is almost in a diagonal form. For case presently under discussion, we are going to perform similar transformation. We define $L(kT)$, $P(kT)$, and $\mathcal{T}(kT)$ as in Chapter 5:

- $L(kT) = -\bar{f}_2 T + \mathcal{O}(T^2)$,
- $P(kT) = \frac{1}{g(kT)c_0} + \mathcal{O}(T)$,
- $\mathcal{T}(kT) = \begin{bmatrix} 1 & -P(kT) \\ -L(kT) & 1 + P(kT)L(kT) \end{bmatrix}$,

and let

$$\mathcal{P}(kT) := \begin{bmatrix} \mathcal{T}(kT) & 0 \\ 0 & I \end{bmatrix} \quad \text{and} \quad \mathcal{P}^{-1}(kT) := \begin{bmatrix} \mathcal{T}^{-1}(kT) & 0 \\ 0 & I \end{bmatrix},$$

and

$$\Lambda(kT) := \mathcal{P}^{-1}(kT) A_{cl}(kT) \mathcal{P}(kT),$$

then the state equation of (6.5) becomes:

$$\begin{aligned} x[(k+1)T] &= \mathcal{P}(kT)\Lambda(kT)\mathcal{P}^{-1}(kT)x(kT) + B_{cl}(kT)n(kT), \\ \mathcal{P}^{-1}(kT)x[(k+1)T] &= \Lambda(kT)\underbrace{\mathcal{P}^{-1}(kT)x(kT)}_{=:\bar{x}(kT)} + \mathcal{P}^{-1}(kT)B_{cl}(kT)n(kT). \end{aligned}$$

This means that

$$\begin{aligned} \bar{x}[(k+1)T] &= \mathcal{P}^{-1}[(k+1)T]x[(k+1)T] \\ &= \big[\Lambda(kT) + \underbrace{(\mathcal{P}^{-1}[(k+1)T]\mathcal{P}(kT) - I)\Lambda(kT)}_{:=\Delta_1(kT)}\big]\bar{x}(kT) + \\ &\quad \big[\mathcal{P}^{-1}(kT)B_{cl}(kT) + \underbrace{(\mathcal{P}^{-1}[(k+1)T] - \mathcal{P}^{-1}(kT))B_{cl}(kT)}_{:=\Delta_2(kT)}\big]n(kT). \end{aligned}$$

Denote $\bar{A}_{cl}(kT) := \Lambda(kT) + \Delta_1(kT)$ and $\bar{B}_{cl}(kT) := \mathcal{P}^{-1}(kT)B_{cl}(kT) + \Delta_2(kT)$, so that the state equation becomes

$$\bar{x}[(k+1)T] = \bar{A}_{cl}(kT)\bar{x}(kT) + \bar{B}_{cl}(kT)n(kT).$$

Using the fact that all the plant parameters have uniformly bounded derivatives (*Assumption 3*), we have:

$$\begin{aligned}
\Lambda(kT) &= \mathcal{P}^{-1}(kT)A_{cl}(kT)\mathcal{P}(kT) \\
&= \begin{bmatrix} 1+\bar{f}_2 T+\mathcal{O}(T^2) & 0 & \frac{T}{g(kT)c_0}c_1(kT)+\mathcal{O}(T^2) \\ 0 & 1-g(kT)c_0+\mathcal{O}(T) & c_1(kT)T+\mathcal{O}(T^2) \\ \mathcal{O}(T^2) & \mathcal{O}(T) & I+A_1(kT)T+\mathcal{O}(T^2) \end{bmatrix}, \\
\Delta_1(kT) &= (\mathcal{P}^{-1}[(k+1)T]\mathcal{P}(kT)-I)\Lambda(kT) \\
&= \begin{bmatrix} \mathcal{O}(T^2) & \mathcal{O}(T) & \mathcal{O}(T^2) \\ \mathcal{O}(T^2) & \mathcal{O}(T^2) & \mathcal{O}(T^3) \\ 0 & 0 & 0 \end{bmatrix}, \\
\mathcal{P}^{-1}(kT)B_{cl}(kT) &= \begin{bmatrix} \mathcal{O}(T) \\ -g(kT)c_0+\mathcal{O}(T) \\ \mathcal{O}(T) \end{bmatrix}, \text{ and} \\
\Delta_2(kT) &= (\mathcal{P}^{-1}[(k+1)T]-\mathcal{P}^{-1}(kT))B_{cl}(kT) \\
&= \begin{bmatrix} \mathcal{O}(T) \\ \mathcal{O}(T^2) \\ 0 \end{bmatrix}.
\end{aligned}$$

The output equation of (6.5) is

$$\begin{aligned}
y(kT) &= C_{cl}(kT)x(kT) \\
&= \underbrace{C_{cl}(kT)\mathcal{P}(kT)}_{=:\bar{C}_{cl}(kT)}\underbrace{\mathcal{P}^{-1}(kT)x(kT)}_{=:\bar{x}(kT)},
\end{aligned} \tag{6.6}$$

with

$$\bar{C}_{cl}(kT) = C_{cl}(kT)\mathcal{P}(kT) = \begin{bmatrix} \mathcal{O}(T) & 1+\mathcal{O}(T) & 0 \end{bmatrix}. \tag{6.7}$$

In addition, the initial condition is $\bar{x}(0) = \mathcal{P}^{-1}(0)x(0) = 0$. From the above, with state $\bar{x}(kT) := \begin{pmatrix} \bar{x}_1(kT) \\ \bar{x}_2(kT) \\ \bar{w}(kT) \end{pmatrix}$ and state matrices

$$\begin{aligned}
\bar{A}_{cl}(kT) &= \begin{bmatrix} 1 + \bar{f}_2 T + \mathcal{O}(T^2) & \mathcal{O}(T) & \frac{T}{g(kT)c_0} c_1(kT) + \mathcal{O}(T^2) \\ \mathcal{O}(T^2) & 1 - g(kT)c_0 + \mathcal{O}(T) & c_1(kT)T + \mathcal{O}(T^2) \\ \mathcal{O}(T^2) & \mathcal{O}(T) & I + A_1(kT)T + \mathcal{O}(T^2) \end{bmatrix}, \\
\bar{B}_{cl}(kT) &= \begin{bmatrix} \mathcal{O}(T) \\ -g(kT)c_0 + \mathcal{O}(T) \\ \mathcal{O}(T) \end{bmatrix}, \text{ and} \\
\bar{C}_{cl}(kT) &= \begin{bmatrix} \mathcal{O}(T) & 1 + \mathcal{O}(T) & 0 \end{bmatrix}.
\end{aligned}$$

the state-space representation of the system is

$$\begin{aligned}
\bar{x}[(k+1)T] &= \bar{A}_{cl}(kT)\bar{x}(kT) + \bar{B}_{cl}(kT)n(kT), \quad \bar{x}(0) = 0, \\
y(kT) &= \bar{C}_{cl}(kT)\bar{x}(kT).
\end{aligned} \tag{6.8}$$

For notation simplicity, we also denote:

$$\begin{aligned}
\bar{A}_{cl}(kT) &=: \begin{bmatrix} A_{11}(kT) & A_{12}(kT) & A_{13}(kT) \\ A_{21}(kT) & A_{22}(kT) & A_{23}(kT) \\ A_{31}(kT) & A_{32}(kT) & A_{33}(kT) \end{bmatrix}, \\
\bar{B}_{cl}(kT) &=: \begin{bmatrix} B_1(kT) \\ B_2(kT) \\ B_3(kT) \end{bmatrix}.
\end{aligned}$$

6.2 Analyzing the LTV System

Since the plant is 'almost' separated into a first order linear time-varying plant and the zero dynamics, we would like to utilize the approach used in Chapter 5. In particular, notice that the first 2 by 2 subsystem (i.e. $\begin{bmatrix} A_{11}(kT) & A_{12}(kT) \\ A_{21}(kT) & A_{22}(kT) \end{bmatrix}$) is exactly the same as $\bar{A}_{cl}(kT)$ from Chapter 5.

In Chapter 5, we could immediately conclude stability; here, this requires more work. In the following, we assume $\bar{x}(0) = 0$ and $n \in PC_\infty$ is arbitrary.

6.2.1 Step 1: Stability

From **Claim 2** of Chapter 5, there exists an $\tilde{f}_2 < 0$ so that for small T

$$\|\bar{A}_{cl}(kT)\| \leq e^{\tilde{f}_2 T}. \tag{6.9}$$

Hence, with zero initial condition we have

$$\begin{pmatrix} \bar{x}_1 \\ \bar{x}_2 \end{pmatrix}[(k+1)T] = \bar{A}_{cl}(kT)\begin{pmatrix} \bar{x}_1 \\ \bar{x}_2 \end{pmatrix}(kT) + \begin{bmatrix} B_1(kT) \\ B_2(kT) \end{bmatrix} n(kT) + \begin{bmatrix} \mathcal{O}(T) \\ \mathcal{O}(T) \end{bmatrix} w(kT).$$

If we regard both n and w as exogenous inputs, by linearity, we can use (5.20) and (5.24) to get a bound on the effect of n; we can use (6.9) to obtain a bound on the effect of w. Using the above arguments, we conclude that there exists a constant $\gamma_{10} > 0$ such that for small T:

$$\|\bar{x}_1(kT)\| = \gamma_{10}\|n\|_\infty + \gamma_{10} \max_{0\leq j\leq k} \|w(jT)\|, \tag{6.10}$$

$$\|\bar{x}_2(kT)\| = (1+\gamma_{10}T)\|n\|_\infty + \gamma_{10} \max_{0\leq j\leq k} \|w(jT)\|, \quad \in \mathbb{Z}^+. \tag{6.11}$$

From Assumption 5, we assume that the zero dynamics of the plant is uniformly exponentially stable. Since $A_{33}(kT)$ is the discrete version of $A_1(t)$, we have that for small T,

$$\begin{aligned} \|\Phi_{A_{33}}[kT, k_0T]\| &\leq \gamma_0 e^{\lambda_0(k-k_0)T} \\ &= \gamma_0\big(e^{\lambda_0 T}\big)^{k-k_0} \\ &= \gamma_0\big(1+\lambda_0 T + \mathcal{O}(T^2)\big)^{k-k_0} \\ &\leq \gamma_0\big(1+\frac{\lambda_0 T}{2}\big)^{k-k_0}, \quad k \geq k_0 \geq 0. \end{aligned} \tag{6.12}$$

Since $A_{31} = \mathcal{O}(T^2)$, $A_{32}(kT) = \mathcal{O}(T)$, and $B_3(kT) = \mathcal{O}(T)$, then with zero initial conditions, it follows from the update equation for $\bar{w}(kT)$ that

$$\begin{aligned}
\|\bar{w}(kT)\| &\leq \Bigg\| \sum_{i=0}^{k-1} \Phi_{A_{33}}\left[[(k-1)T],[(k-i)T]\right] \Big\{ A_{31}[(k-i-1)T]\bar{x}_1[(k-i-1)T] + \\
&\quad A_{32}[(k-i-1)T]\bar{x}_2[(k-i-1)T] + B_3[(k-i-1)T]n[(k-i-1)T] \Big\} \Bigg\| \\
&\leq \gamma_0 \Bigg| \sum_{i=0}^{k-1} \big(1 + \frac{\lambda_0 T}{2}\big)^i \Bigg| \Big(\mathcal{O}(T^2) \max_{0\leq j\leq k} \|\bar{x}_1(jT)\| + \mathcal{O}(T) \max_{0\leq j\leq k} \|\bar{x}_2(jT)\| + \\
&\quad \mathcal{O}(T)||n||_\infty \Big) \qquad (6.13) \\
&= \mathcal{O}(T) \max_{0\leq j\leq k} \|\bar{x}_1(jT)\| + \mathcal{O}(1) \max_{0\leq j\leq k} \|\bar{x}_2(jT)\| + \mathcal{O}(1)\|n\|_\infty.
\end{aligned}$$

Hence, there exists a constant $\gamma_{11} \geq \gamma_{10}$ such that for small T,

$$\|\bar{w}(kT)\| = \gamma_{11} T \max_{0\leq j\leq k} \|\bar{x}_1(jT)\| + \gamma_{11} \max_{0\leq j\leq k} \|\bar{x}_2(jT)\| + \gamma_{11}\|n\|_\infty, \quad k \in \mathbb{Z}^+. \qquad (6.14)$$

Since the RHS of (6.10), (6.11), and (6.14) are monotonically increasing, we can conclude that for small T:

$$\begin{aligned}
\max_{0\leq j\leq k} \|\bar{x}_1(jT)\| &\leq \gamma_{11}\|n\|_\infty + \gamma_{11} \max_{0\leq j\leq k} \|\bar{w}(jT)\|, \qquad (6.15) \\
\max_{0\leq j\leq k} \|\bar{x}_2(jT)\| &\leq (1+\gamma_{11}T)\|n\|_\infty + \gamma_{11} \max_{0\leq j\leq k} \|\bar{w}(jT)\|, \qquad (6.16) \\
\max_{0\leq j\leq k} \|\bar{w}(jT)\| &\leq \gamma_{11}\|n\|_\infty + \gamma_{11} T \max_{0\leq j\leq k} \|\bar{x}_1(jT)\| + \\
&\quad \gamma_{11} \max_{0\leq j\leq k} \|\bar{x}_2(jT)\|, \quad k \in \mathbb{Z}^+. \qquad (6.17)
\end{aligned}$$

Substituting (6.15) into (6.17) we see that for small T, we have the following implicit bound:

$$\max_{0\leq j\leq k} \|\bar{w}(jT)\| \leq \gamma_{11}\|n\|_\infty + \gamma_{11}^2 T\|n\|_\infty + \gamma_{11}^2 T \max_{0\leq j\leq k} \|\bar{w}(jT)\| + \gamma_{11} \max_{0\leq j\leq k} \|\bar{x}_2(jT)\|, k \geq 0.$$

Hence, there exists a constant γ_{12} such that for small T:

$$\begin{aligned}
\max_{0\leq j\leq k} \|\bar{w}(jT)\| &\leq \gamma_{12}\|n\|_\infty + \gamma_{12} \max_{0\leq j\leq k} \|x_2(jT)\|, \qquad (6.18) \\
\max_{0\leq j\leq k} \|\bar{x}_1(jT)\| &\leq \gamma_{12}\|n\|_\infty + \gamma_{12} \max_{0\leq j\leq k} \|x_2(jT)\|. \qquad (6.19)
\end{aligned}$$

Now we need to look at the update equation for $\bar{x}_2$. By using the fact that for small T:

$$|1 - g(kT)c_0 + \mathcal{O}(T)| \leq 1 - \frac{1-\varepsilon}{2},$$

we see that there exist a constant $\gamma_{13} \geq \gamma_{12}$ such that

$$\|\bar{x}_2(kT)\| \leq \gamma_{13}T^2 \max_{0\leq j\leq k} \|\bar{x}_1(jT)\| + \gamma_{13}T \max_{0\leq j\leq k} \|\bar{w}(jT)\| + \gamma_{13}\|n\|_\infty, k \geq 0.$$

Using (6.18) and (6.19) in the above equation yields

$$\begin{aligned}\sup_{0\leq j\leq k} \|\bar{x}_2(jT)\| &\leq \gamma_{13}T^2 \max_{0\leq j\leq k} \|\bar{x}_1\| + \gamma_{13}T \max_{0\leq j\leq k} \|\bar{w}(jT)\| + \gamma_{13}\|n\|_\infty \\ &\leq (\gamma_{13} + \gamma_{12}\gamma_{13}T + \gamma_{12}\gamma_{13}T^2)\|n\|_\infty + (\gamma_{12}\gamma_{13}T + \gamma_{12}\gamma_{13}T^2) \max_{0\leq j\leq k} \|\bar{x}_2(jT)\|,\end{aligned}$$

so there exist a positive constant γ_{14} such that for sufficient small T:

$$\sup_{0\leq j\leq k} \|\bar{x}_2(jT)\| \leq \gamma_{14}\|n\|_\infty, k \geq 0,$$

so

$$\sup_{j\geq 0} \|\bar{x}_2(jT)\| \leq \gamma_{14}\|n\|_\infty, k \geq 0, \tag{6.20}$$

as well. If we substitute the above into (6.18) and (6.19), we see that

$$\sup_{j\geq 0} \|\bar{w}(jT)\| \leq (\gamma_{12}\gamma_{14} + \gamma_{12})\|n\|_\infty, \tag{6.21}$$

$$\sup_{j\geq 0} \|\bar{x}_1(jT)\| \leq (\gamma_{12}\gamma_{14} + \gamma_{12})\|n\|_\infty. \tag{6.22}$$

Hence, we have stability.

6.2.2 Step 2: Tighter bound

Now, we will utilize the approach of Chapter 5 to obtain a tighter bound on the state $\bar{x}_2$. Combining (6.22) and (6.21) with the update equation for $\bar{x}_2$ we have

$$\begin{aligned}\bar{x}_2[(k+1)T] &= [1 - g(kT)c_0 + \mathcal{O}(T)]\bar{x}_2(kT) + \mathcal{O}(T^2)\|n\|_\infty + \mathcal{O}(T)\|n\|_\infty + \\ &\quad [-g(kT)c_0 + \mathcal{O}(T)]\|n\|_\infty \\ &= [1 - g(kT)c_0]\bar{x}_2(kT) + [-g(kT)c_0 n(kT)] + \underbrace{\mathcal{O}(T)\bar{x}_2(kT) + \mathcal{O}(T)\|n\|_\infty}_{=:\Delta_4(kT)}.\end{aligned} \tag{6.23}$$

The above equation is essentially the same as (5.21) of Chapter 5. Using exactly the same argument, it follows that

$$\sup_{k\geq 0} \|\bar{x}_2(kT)\| = (1+\mathcal{O}(T))\|n\|_\infty. \tag{6.24}$$

6.2.3 Induced Noise Gain (For relative degree one case)

Using the result from (6.22), (6.24), and (6.21) and substituting into (6.6), we have

$$\begin{aligned} |y(kT)| &= |\bar{C}_{cl}(kT)\bar{x}(kT)| \\ &= \mathcal{O}(T)\sup_{k\geq 0}\|\bar{x}_1(kT)\| + (1+\mathcal{O}(T))\sup_{k\geq 0}\|\bar{x}_2(kT)\| \\ &= (1+\mathcal{O}(T))\,||n||_\infty, \quad k\in\mathbb{Z}^+, \end{aligned} \tag{6.25}$$

which implies that the output is well behaved at the sample points.

Now, we will show that the output is also well behaved in between the sample points.

Since $x(kT) = \mathcal{P}(kT)\bar{x}(kT)$, if we use the bound found for $\bar{x}$, we have

$$\begin{aligned} x(kT) &= \begin{pmatrix} 1 & -\frac{1}{g(kT)c_0}+\mathcal{O}(T) & 0 \\ \bar{f}_2T+\mathcal{O}(T^2) & 1-\frac{\bar{f}_2T}{g(kT)c_0}+\mathcal{O}(T^2) & 0 \\ 0 & 0 & I \end{pmatrix} \begin{pmatrix} \mathcal{O}(1) \\ 1+\mathcal{O}(T) \\ \mathcal{O}(1) \end{pmatrix} \|n\|_\infty, \\ &= \begin{pmatrix} \mathcal{O}(1) \\ 1+\mathcal{O}(T) \\ \mathcal{O}(1) \end{pmatrix} \|n\|_\infty, \quad k\geq 0, \end{aligned}$$

so in particular,

$$x_1(kT) = \mathcal{O}(1)\|n\|_\infty. \tag{6.26}$$

Substituting the above result into the state-space output equation of the controller (4.7), we have

$$u(kT) = \mathcal{O}(1)\|n\|_\infty + \frac{1}{T}(-c_0)\left(y(kT)+n(kT)\right), \quad k\geq 0.$$

Substituting the result of (6.25) into the above equation, it follows that

$$\begin{aligned} \sup_{k\geq 0}|u(kT)| &= \mathcal{O}(T)\|n\|_\infty + \mathcal{O}\left(\tfrac{1}{T}\right)\left[(1+\mathcal{O}(T))\|n\|_\infty + \|n\|_\infty\right] \\ &= \mathcal{O}\left(\tfrac{1}{T}\right)\|n\|_\infty. \end{aligned} \tag{6.27}$$

As in Chapter 5, the bound on the control input is inversely proportional to the sampling period. Sampling faster could cause a large control signal, which is the case in practice. Now, let's look at the continuous time relative degree one plant equation (6.2). Let $\Phi_{A_{pc}}$ denote the transition matrix, we have that for any $t \in [kT, (k+1)T)$,

$$\begin{pmatrix} w(t) \\ v(t) \end{pmatrix} = \Phi_{A_{pc}}(t, kT) \begin{pmatrix} w(kT) \\ v(kT) \end{pmatrix} + \int_{kT}^{t} \Phi_{A_{pc}}(t, \tau) B_{pc}(\tau) u(\tau) d\tau. \tag{6.28}$$

Since we are using the sample-data controller, we have for $t \in [kT, (k+1)T)$, $u(t) = u(kT)$. Since every element of A_{pc} and B_{pc} lies in a compact set $\bar{\Gamma}$, there exist constants γ_{13} and γ_{14} such that

$$\|A_{pc}\|_\infty \leq \gamma_{13} \quad \text{and} \quad \|B_{pc}\|_\infty \leq \gamma_{14}.$$

It is easy to see that

$$\Phi_{A_{pc}}(t, \tau) = I + \mathcal{O}(T), \quad kT \leq \tau \leq t \leq (k+1)T, \quad k \in \mathbb{Z}^+.$$

Applying Lemma 2 from Appendix B, we have

$$B_{pc}(\tau) = B_{pc}(kT) + \mathcal{O}(T).$$

Using the above results in (6.28), we end up with

$$\begin{pmatrix} w(t) \\ v(t) \end{pmatrix} = (I + \mathcal{O}(T)) \begin{pmatrix} w(kT) \\ v(kT) \end{pmatrix} + (t - kT)(B_{pc}(kT) + \mathcal{O}(T))u(kT). \tag{6.29}$$

Since $y(t) = v(t)$ and $B_{pc}(kT) = \begin{bmatrix} 0 \\ \vdots \\ 0 \\ g(t) \end{bmatrix}$, we have

$$\begin{aligned} y(t) &= (I + \mathcal{O}(T))y(kT) + (t - kT)(g(kT) + \mathcal{O}(T))u(kT) \\ &= [y(kT) + (t - kT)g(kT)u(kT)] + [\mathcal{O}(T)y(kT) + (t - kT)\mathcal{O}(T)u(kT)]. \end{aligned}$$

The above equation is exactly the same as (5.27) of Chapter 5. Hence, using exactly the same argument, we conclude that the output is well behaved between the sample points and

$$\|y\|_\infty = (1 + \mathcal{O}(T))\|n\|_\infty. \tag{6.30}$$

Since $n \in PC_\infty$ is arbitrary, it follows that

$$\|T_{ny}\| = 1 + \mathcal{O}(T).$$

Finally, we present our main result.

Proposition 3. *For a relative degree one time-varying plant of the form (6.2) with known sign of the high frequency gain, using controller (3.21)-(3.25), the maximum induced noise gain is bounded. In particular, if the selection of c_0 satisfies $\bar{g}c_0 \in (0,1)$, then for every $\delta > 0$, there exists a $\bar{T} > 0$ such that for every $T \in (0,\bar{T})$ and $\bar{\theta}(t) \in \bar{\mathcal{P}}_{ac}(n, m = 1, \bar{\Gamma}, \bar{\mu}_1, \underline{g}, \gamma_0, \lambda_0)$ for all $t \geq 0$, we have*

$$\|T_{ny}(\bar{\theta}, T)\| \leq 1 + \delta. \tag{6.31}$$

In this chapter, we leveraged some Chapter 5's results to assist our new proof. As expected, the induced noise gain is the same as in the previous chapters.

6.3 Simulation Result

To illustrate the noise behavior for relative degree one case, a simulation is presented here. In this simulation, we use the same reference model, modeled inputs, and anti-aliasing filter as presented in (4.27), (4.28), and (4.29). Here, we choose the plant to be second order but with relative degree one. The plant is chosen to be:

$$\begin{aligned}
\dot{x}(t) &= \begin{bmatrix} 0 & 1 \\ a_0(t) & a_1(t) \end{bmatrix} x(t) + \begin{bmatrix} 0 \\ g(t) \end{bmatrix} u(t), \\
y(t) &= \begin{bmatrix} 0 & 1 \end{bmatrix} x(t),
\end{aligned}$$

with

$$\begin{aligned}
a_0(t) &= 2\cos(t), \\
a_1(t) &= 4\cos(t/2), \quad \text{and} \\
g(t) &= 1.5 + 1.2\sin(\frac{t}{2}).
\end{aligned}$$

We choose $c_0 = \frac{1}{3}$ so that $g(t)c_0 \in [0.1, 0.9]$ for all $t \geq 0$. We inject noise at the measurement of the plant output. To make the noise behavior more visualizable, we choose large random noise signals such that $||n||_\infty = 1$. The initial condition of the output is set to be $y(0) = 0$. The simulation is shown in Figure (6.1).

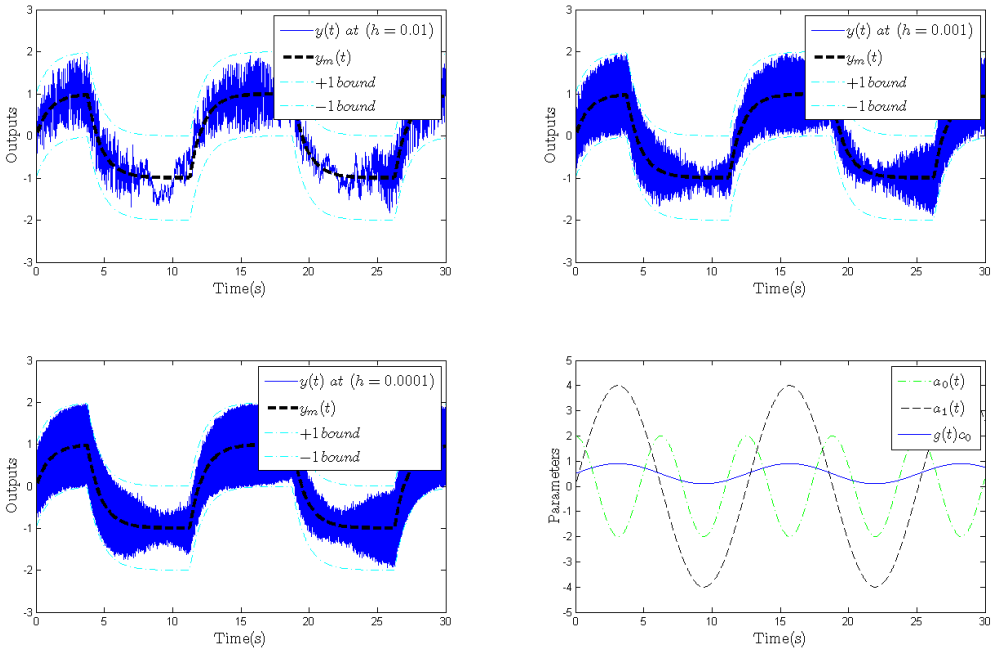

Figure 6.1: Relative degree one plant simulation with different sampling period

The first three figures plot the modeled output 'y_m' and the plant outputs 'y' with sampling period h being 0.01s, 0.001s and 0.0001s, respectively. The last plot shows the time-varying plant parameters. As we can see, as the sampling period gets smaller, the output appears to be more "noisy". More importantly, we see that all the plant outputs are within the ± 1 bound. This confirms our proven result.

Chapter 7

Conclusion

In this thesis, we analyzed the noise rejection of the MRAC in Miller [1]. For the sampled-data system in [1], we investigated the cases where the plant is first order LTI, first order LTV, and LTV with relative degree one. For each of the above cases, we found an expression for the induced noise gain as a function of a key controller parameter c_0 and provided a range for which the noise performance is good. We provided detailed derivations and proofs of the expression of the induced noise gain.

It was found that to improve the noise rejection of our sampled-data control system, we first have to assume that the sign of the high frequency gain is known. This assumption is one of the classical assumptions on the plant model for the MRACP. More importantly, we also found that the controller parameter c_0 has direct impact on the induced noise gain. To improve noise rejection, we add more restrictions to the range of c_0. Sacrificing about half of the allowed range of c_0 (that is specified in [1]), we ensured that the induced noise gain is always $1 + \mathcal{O}(T)$.

Adding assumptions on the sign of the high frequency gain and embracing a mild restriction on the selection of the control parameter c_0, the sampled-data controller in [1] now has the following properties:

- the controller is linear; control signal is modest in size,
- it can handle rapidly time-varying plant parameters,
- tracking is immediate rather than asymptotic,
- extremely good noise rejection if the relative degree of the plant is one.

These desirable properties of the noise rejection made the controller more practical (since measurement noise naturally exists in real-life applications).

In this thesis, the result ensured good noise rejection for LTV relative degree one plants. However, the result would be much stronger if we can extend to plants with higher relative degree. In the view of the author, this might require modifications to the structure of the controller. We will leave this as the future work.

APPENDICES

Appendix A

List of Notations

Since this thesis contains a significant amount of notations, we will compile the important terms with descriptions provided. Although it may sometimes be repetitive, to improve accessibility, we will present the list of the notations according to the corresponding chapters.

Table A.1: Notation for Chapter 3

Symbol	(**Eq./page#**)	**Description**
n	(3.1)	Order of the plant.
m	(3.1)	Relative degree of the plant.
h	p.8	Sampling period.
T	p.8	Control period. Depending on the relative degree of the plant, one control period could consist multiple sampling periods (i.e. $T = mh$).
P_m	(3.3)	The stable reference plant.
(A_m, B_m, C_m)	(3.3)	State matrices of P_m.
F_α	(3.4)	Anti-aliasing filter, where $\bar{u}_m = \sigma\bar{u}_m + \sigma u_m$, $\bar{u}_m(t_0) = \bar{u}_{m_0}$, and $\sigma > 0$.
$\bar{e}$	(3.6)	Tracking error, where $\bar{e}(t) := \bar{y}_m(t) - y(t)$.
w, v	p.9	States of the general plant, where w is associated with the zero dynamics and v is associated with the output y and its derivatives.
$\bar{\theta}$	(3.12)	A compact set where $\theta \in PS_\infty$. The state-space model of the general plant is parametrized by $\bar{\theta}$.

$\bar{\mathcal{P}}$	(3.13)	The set of plant uncertainties.
u^o	(3.18)	The ideal control signal.
$\hat{u}^o$	(3.21)-(3.25)	Estimated ideal control signal.
γ_m, λ_m	p.9	Parameters of the reference plant. $\gamma_m > 0$ and $\lambda_m < 0$ are chosen so that $\|e^{A_m t}\| \leq \gamma_m e^{\lambda_m t}$.
$\bar{f}_2$	(3.18)	Control parameter. $\bar{f}_2$ need to be chosen so that $\bar{A}_2 = \Lambda_2 + b_2 \bar{f}_2$ is stable and has eigenvalue with real parts less than λ_m.
$\underline{g}$,$\bar{g}$	p.20	Positive constant such that the high frequency gain $g(t) \in [\underline{g}, \bar{g}]$ for all $t \geq 0$.
$n(kT)$	p.22	Measurement noise on the plant output at time $t = kT$.
$y_n(kT)$	p.22	Measured plant output at $t = kT$. $y_n(kT) := y(kT) + n(kT)$, where $y(kT)$ is the real plant output

Table A.2: Notation for Chapter 4

Symbol	**Eq./page#**	**Description**
(A_c, B_c, C_c, D_c)	(4.7)	The state-space matrices corresponding to the controller.
(A_p, B_p, C_p, D_p)	(4.8)	The state-space matrices corresponding to the first order LTI plant.
$(A_{cl}, B_{cl}, C_{cl}, D_{cl})$	(4.9)	The state-space matrices of the closed-loop system when connecting the controller with a first order LTI plant.
L, P	(4.10,4.14)	Used to perform a similarity transformation which diagonalize A_{cl}.
$\mathcal{T}$	4.15	Similarity transformation matrix which diagonalize A_{cl}, where $\mathcal{T} := \begin{bmatrix} 1 & 0 \\ -L & 1 \end{bmatrix} \begin{bmatrix} 1 & -P \\ 0 & 1 \end{bmatrix}$.

$(\bar{A}_{cl}, \bar{B}_{cl}, \bar{C}_{cl})$	p.30,31	The state-space matrices of the closed-loop system after performing similarity transformation. $\bar{A}_{cl}$ is diagonal.
$h(\cdot)$	(4.15)	The impulse response.
λ_1,λ_2	(4.16)	The two eigenvalues of $\bar{A}_{cl}$.

Table A.3: Notation for Chapter 5

Symbol	**Eq./page#**	**Description**
ε	p.38	A fixed positive constant. We set $\varepsilon = 1 - \underline{g}c_0$ so that $\lvert 1 - gc_0 \rvert \leq \varepsilon < 1$.
$\begin{pmatrix} A_p(kT) & B_p(kT) \\ C_p(kT) & D_p(kT) \end{pmatrix}$	(5.3)	The state-space matrices of the the first order LTV plant.
$\begin{pmatrix} A_{cl}(kT) & B_{cl}(kT) \\ C_{cl}(kT) & D_{cl}(kT) \end{pmatrix}$	(5.5)	The state-space matrices of the closed-loop system when connecting the controller with a first order LTV plant.
$L(kT), P(kT)$	(5.5)	Used to perform a similarity transformation which diagonalize $A_{cl}(kT)$. Note that both $L(kT)$ and $P(kT)$ are time-varying.
$\mathcal{T}(kT)$	(5.5)	Similarity transformation matrix which diagonalize A_{cl}, where $\mathcal{T}(kT) = \begin{bmatrix} 1 & 0 \\ -L(kT) & 1 \end{bmatrix} \begin{bmatrix} 1 & -P(kT) \\ 0 & 1 \end{bmatrix}$.
$\Lambda(kT)$ $\Delta_1(kT)$ $\Delta_2(kT)$	(5.7)	Matrices used to define the state matrices of the $\bar{x}$ system, where $\Lambda(kT) = \mathcal{T}^{-1}(kT)A_{cl}(kT)\mathcal{T}(kT)$, $\Delta_1(kT) = (\mathcal{T}^{-1}[(k+1)T]\mathcal{T}(kT) - I)\Lambda(kT)$, $\Delta_2(kT) = (\mathcal{T}^{-1}[(k+1)T] - \mathcal{T}^{-1}(kT))B_{cl}(kT)$.

$\bar{A}_{cl}(kT)$ $\bar{B}_{cl}(kT)$ $\bar{C}_{cl}(kT)$	(5.10)	The state-space matrices of the closed-loop system after performing similarity transformation, where $\bar{A}_{cl}(kT) = \Lambda(kT) + \Delta_1(kT),$ $\bar{B}_{cl}(kT) = \mathcal{T}^{-1}(kT)B_{cl}(kT) + \Delta_2(kT),$ $\bar{C}_{cl}(kT) = C_{cl}(kT)\mathcal{T}(kT).$
$\tilde{f}_2$	p.43	A negative constant. It is used when proving stability.

Table A.4: Notation for Chapter 6

Symbol	**Eq./page#**	**Description**
$(A_{pc}(t), B_{pc}(t), C_{pc}(t))$	(6.2)	The c.t. state-space matrices of the relative degree one plant.
$(A_p(kT), B_p(kT), C_p(kT))$	(6.4)	The d.t. state-space matrices of the relative degree one plant.
$(A_{cl}(kT), B_{cl}(kT), C_{pc}(kT))$	(6.5)	The state-space matrices of the closed-loop system when connecting the controller with the relative degree one LTV plant.
$\mathcal{P}(kT)$	p.55	Similarity transformation matrix. $\mathcal{P}(kT) = \begin{bmatrix} \mathcal{T}(kT) & 0 \\ 0 & I \end{bmatrix}.$
$\Lambda(kT)$ $\Delta_1(kT)$ $\Delta_2(kT)$	p.56	Matrices used to define the state matrices of the $\bar{x}$ system, where $\Lambda(kT) = \mathcal{P}^{-1}(kT)A_{cl}(kT)\mathcal{P}(kT),$ $\Delta_1(kT) = (\mathcal{P}^{-1}[(k+1)T]\mathcal{P}(kT) - I)\Lambda(kT),$ $\Delta_2(kT) = (\mathcal{P}^{-1}[(k+1)T] - \mathcal{P}^{-1}(kT))B_{cl}(kT).$

$\bar{A}_{cl}(kT)$ $\bar{B}_{cl}(kT)$ $\bar{C}_{cl}(kT)$	(6.8)	The state-space matrices of the closed-loop system after performing similarity transformation, where $\bar{A}_{cl}(kT) = \Lambda(kT) + \Delta_1(kT),$ $\bar{B}_{cl}(kT) = \mathcal{P}^{-1}(kT)B_{cl}(kT) + \Delta_2(kT),$ $\bar{C}_{cl}(kT) = C_{cl}(kT)\mathcal{P}(kT).$

Appendix B

Proofs

Before starting the proofs, two technical results are presented which are used in other proofs. In these results, $A(t)$ is a time-varying square matrix and $B(t)$ is a time-varying matrix with dimension $n \times m$. We let Φ_A denote the transition matrix corresponding to A.

Lemma 1. *[3]: Consider the differential equation*

$$\dot{\eta}(t) = A(t)\eta(t)$$

with $A \in PC_\infty$ and $c := ||A||_\infty$. Then, for $t \geq t_0$,

$$\begin{aligned} \|\Phi_A(t, t_0)\| &\leq e^{c(t-t_0)}, \\ \|\Phi_A(t, t_0) - I\| &\leq (e^{c(t-t_0)} - 1). \end{aligned}$$

Lemma 2. *: Consider a time-varying matrix $B(t)$ of dimension $n \times m$, where $n \geq m \geq 1$. If $B \in PC_\infty$ and $\gamma := \|\dot{B}\|_\infty$, then for all $k \geq 0$, and $t \in [kT, (k+1)T)$,*

$$B(t) = B(kT) + \mathcal{O}(T).$$

Proof. At any time $t \in [kT, (k+1)T)$,

$$B(t) = B(kT) + \int_{kT}^{t} \dot{B}(\tau) d\tau.$$

Then

$$\begin{aligned} ||B(t) - B(kT)|| &= \left\| \int_{kT}^{t} \dot{B}(\tau) d\tau \right\| \\ &\leq \int_{kT}^{t} \left\| \dot{B}(\tau) \right\| d\tau \\ &\leq \gamma(t - kT) \\ &\leq \gamma T. \end{aligned}$$

This means that

$$B(t) - B(kT) = \mathcal{O}(T),$$

or

$$B(t) = B(kT) + \mathcal{O}(T).$$

□

Lemma 3. *For $A \in \mathbb{R}^{n \times n}$ and $B \in \mathbb{R}^{n \times 1}$, if every element of $A(t)$ and $B(t)$ is absolutely continuous and satisfies:*

- $\|A\|_\infty \leq c_1$, $c_1 > 0$,
- $\|B\|_\infty \leq \bar{g}$,
- $\|\dot{A}\|_\infty \leq \bar{\mu}_1$,
- $\|\dot{B}\|_\infty \leq \bar{\mu}_1$,

then the linear time-varying system:

$$\dot{x}(t) = A(t)x(t) + B(t)u(t), \quad x(0) = 0, \tag{B.1}$$

with

$$u(t) = u(kT), \quad kT \leq t < (k+1)T, \ k \in \mathbb{Z}^+,$$

can be discretized as

$$x[(k+1)T] = \Big[1 + A(kT)T + \mathcal{O}(T^2)\Big]x(kT) + \Big[TB(kT) + \mathcal{O}(T^2)\Big]u(kT), \quad k \geq 0.$$

Proof. First, let us consider a slightly different system. For $k \in \mathbb{Z}^+$ and $t \in [kT, (k+1)T]$, consider:

$$\begin{array}{rcl} \dot{\hat{x}}(t) & = & A(kT)\hat{x}(t) + B(kT)u(t), \quad \hat{x}(kT) = x(kT), \\ u(t) & = & u(kT). \end{array} \tag{B.2}$$

Denote the associated transition matrix by

$$\Phi(t, t_0) := e^{A(kT)(t-t_0)}, \quad kT \leq t_0 \leq t \leq (k+1)T,$$

so the solution of (B.2) is

$$\hat{x}(t) = \Phi(t, kT)x(kT) + \left(\int_{kT}^{t} \Phi(\tau, kT)d\tau\right) B(kT)u(kT).$$

Since

- $\|A\|_\infty \leq c_1$, $c_1 > 0$,
- $\|B\|_\infty \leq \bar{g}$,

applying Lemma 1 (from Appendix B) yields

$$\|\hat{x}(t)\| \leq e^{c_1(t-kT)}\|x(kT)\| + (t - kT)e^{c_1(t-kT)}\bar{g}|u(kT)|. \tag{B.3}$$

At $t = (k+1)T$, (B.2) has the solution

$$\hat{x}[(k+1)T] = e^{A(kT)T}x(kT) + \left(\int_0^T e^{A(kT)\tau}d\tau\right) B(kT)u(kT). \tag{B.4}$$

Using Taylor Series expansion with order notation, we have that

$$e^{A(kT)T} = I + A(kT)T + \mathcal{O}(T^2), \tag{B.5}$$

and

$$e^{A(kT)\tau} = I + A(kT)\tau + \mathcal{O}(\tau^2).$$

It follows that

$$\begin{array}{rcl} \int_0^T e^{A(kT)\tau}d\tau & = & \int_0^T Id\tau + A(kT)\int_0^T \tau d\tau + \int_0^T \mathcal{O}(\tau^2)d\tau. \\ & = & IT + A(kT)\mathcal{O}(T^2) + \mathcal{O}(T^3), \end{array}$$

$$\int_0^T e^{A(kT)\tau}d\tau = IT + \mathcal{O}(T^2). \tag{B.6}$$

Use the results of (B.5) and (B.6) in (B.4) yields

$$\hat{x}[(k+1)T] = \big(I + A(kT)T + \mathcal{O}(T^2)\big)\, x(kT) + \big(TB(kT) + \mathcal{O}(T^2)\big)\, u(kT). \tag{B.7}$$

Notice that the above equation carries exactly the same form as the one we want. However, in the $\hat{x}$ system, we are assuming that the state matrices are time invariant within every sampling period. Since every element of $A(t)$ and $B(t)$ is smooth and uniformly bounded, we expect that their variation inside each sampling period has maximum $\mathcal{O}(T^2)$ effect to the system.

Now, for $t \in [kT, (k+1)T]$, let

$$\tilde{x}(t) := x(t) - \hat{x}(t).$$

It follows that

$$\begin{aligned} \dot{\tilde{x}}(t) &= \dot{x}(t) - \dot{\hat{x}}(t) \\ &= A(t)\tilde{x}(t) + (A(t) - A(kT))\hat{x}(t) + (B(t) - B(kT))u(kT). \end{aligned}$$

Since $x(kT) = \hat{x}(kT)$, we have $\tilde{x}(kT) = 0$. Using the fact that

- $\|\dot{A}\|_\infty \le \mu_1$, and
- $\|\dot{B}\|_\infty \le \mu_1$,

then with Lemma 2 (from Appendix B), it follows that:

- $\|A(t) - A(kT)\| \le \mu_1(t - kT)$,
- $\|B(t) - B(kT)\| \le \mu_1(t - kT)$.

Hence, for $t \in [kT, (k+1)T]$, if we denote the state transition matrix of $A(t)$ to be $\Phi_A(t, kT)$, then

$$\|\tilde{x}(t)\| \le \int_{kT}^{t} \|\Phi_A(t, kT)\| \big[\mu_1(\tau - kT)\|\hat{x}(\tau)\| + \mu_1(\tau - kT)|u(kT)|\big] d\tau. \tag{B.8}$$

Applying Lemma 1, we have for $\tau \in [kT, (k+1)T]$,

$$\|\Phi_A(\tau, kT)\| \le e^{c_1(\tau - kT)} \le e^{c_1 T}.$$

Using (B.3) and the above result in (B.8) yields

$$\begin{aligned} \|\tilde{x}(t)\| &\leq \int_{kT}^{t} e^{c_1 T}\Big\{\mu_1(\tau - kT)\big[e^{c_1 T}\|x(kT)\| + \bar{g}(\tau - kT)e^{c_1 T}|u(kT)|\big] + \\ &\quad \mu_1(\tau - kT)|u(kT)|\Big\}d\tau \\ &= \mu_1 e^{2c_1 T}\tfrac{(t-kT)^2}{2}\|x(kT)\| + \bar{g}\mu_1 e^{2c_1 T}\tfrac{(t-kT)^3}{3}|u(kT)| + \\ &\quad \mu_1\tfrac{(t-kT)^2}{2}e^{c_1 T}|u(kT)|. \end{aligned} \tag{B.9}$$

Hence, at $t = (k+1)T$, it follows that

$$\tilde{x}[(k+1)T] = \mathcal{O}(T^2)x(kT) + \mathcal{O}(T^2)u(kT). \tag{B.10}$$

Using the above and (B.7), we can have

$$\begin{aligned} x[(k+1)T] &= \hat{x}[(k+1)T] + \tilde{x}[(k+1)T] \\ &= \left(I + A(kT)T + \mathcal{O}(T^2)\right)x(kT) + \left(TB(kT) + \mathcal{O}(T^2)\right)u(kT). \end{aligned} \tag{B.11}$$

as desired. □

References

[1] Daniel E. Miller and Naghmeh Mansouri, *"Model Reference Adaptive Control Using simultaneous Probing, Estimation, and Control"*. VOL. 55, NO. 9, IEEE Transactions on Automatic Control, SEPTEMBER 2010.

[2] PETAR V. KOKOTOVIĆ, *"A Riccati Equation for Block-Diagonalization of Ill-Conditioned Systems"*. IEEE Trans, VOL. 20, pp. 812-814, Dec. 1975.

[3] Daniel E. Miller, *"A New Approach to Model Reference Adaptive Control"*. IEEE Transactions on Automatic Control, pp. 743-756. May. 2003.

[4] R.W. Brochett and H. B. Lee, *"Frequency-domain instability criteria for time-varying and nonlinear systems."*. Proc. IEEE, vol. 55, pp. 604-619. May. 1967.

[5] G.C. Goodwin and K.S. Sin, *"Adaptive Filtering prediction and Control"*. Prentice Hall, Englewood Cliffs, New Jersey, USA, 1984.

[6] H. P. Whitaker, J. Yamron, and A. Kezer, *"Design of model reference adaptive control systems for aircraft"*. Technical Report R-164, Instrumentation Laboratory, MIT Press, Cambridge, Massachusetts, 1958.

[7] B. Egardt, *"Stability of adaptive controllers"*. Lecture notes in control and Information Science, no. 20, Springer-Verlag, 1979.

[8] G. C. Goodwin, P. J. Ramadge, and P E Caines, *"Discrete time multi-variable control"*. IEEE Transactions on Automatic Control, AC-25:449-456, 1980.

[9] A. S. Morse, *"Global stability of parameter-adaptive control systems"*. IEEE Transactions on Automatic Control, AC-25:433-439, 1980.

[10] K. S. Narendra, Y. H. Lin, and L. S. Valavani, *"Stable adaptive controller design"*, part ii: Proof of stability. IEEE Transactions on Automatic Control, AC-25:440-448, 1980.

[11] G. Tao and P. A. Ioannou, *"Model reference adaptive control for plants with unknown relative degree"* in Proc. Amer. Control Conf., pp. 2297-2302, 1989.

[12] D. R. Mudgett and A. S. Morse, *"Adaptive stabilization of linear systems with unknown high-frequency gains"*, IEEE Trans. Automat. Contr., vol. AC-30, pp. 549-554, 1985.

[13] G. C. Goodwin, D. J. Hill, and X. Xianya, *"Stochastic adaptive control for exponentially convergent time-varying systems"*, Proceedings of the IEEE 23rd Conference on Decision and Control, 23:39-44, 1984.

[14] R. H. Middleton and G. C. Goodwin, *"Adaptive control of time-varying linear systems"*, IEEE Transaction on Automatic Control, 33(2):150-155, 1988.

[15] F. Ohkawa, *"A model reference adaptive control system for a class of discrete linear time varying systems with time delay"*, International Journal of Control, 42(5):1227-1238, 1985.

[16] K. S. Tsakalis and P. A. Ioannou, *"Adaptive control of linear time-varying plants: A new model reference controller structure"*, IEEE Transaction on Automatic Control, 34(10):1038-1046, 1989.

[17] K. S. Tsakalis and P. A. Ioannou, *"Linear Time-Varying Systems"*, Prentice Hall, 1993.

[18] Naghmeh Mansouri, *"On A New Approach to Model Reference Adaptive Control"*, PHD thesis, University of Waterloo, 2008.

[19] Munther A. Dahleh and J. Boyd Pearson *"l^1-Optimal Feedback Controllers for MIMO Discrete-Time Systems"*, IEEE Transaction on Automatic Control, Vol. AC-32, NO. 4, April 1987.